Journal of Advanced Research 30 (2021) 85–102

Contents lists available at ScienceDirect

Journal of Advanced Research

journal homepage: www.elsevier.com/locate/jare

33-kDa ANXA3 isoform contributes to hepatocarcinogenesis *via* modulating ERK, PI3K/Akt-HIF and intrinsic apoptosis pathways

Chunmei Guo [a,1], Nannan Li [b,1], Chengyong Dong [c], Liming Wang [c], Zhaopeng Li [b], Qinlong Liu [c], Qinglai Ma [a], Frederick T. Greenaway [f], Yuxiang Tian [b], Lihong Hao [d], Shuqing Liu [b,*], Ming-Zhong Sun [a,e,*]

[a] *Department of Biotechnology, College of Basic Medical Sciences, Dalian Medical University, Dalian 116044, China*
[b] *Department of Biochemistry, College of Basic Medical Sciences, Dalian Medical University, Dalian 116044, China*
[c] *Department of General Surgery, the 2nd Affiliated Hospital, Dalian Medical University, Dalian 116027, China*
[d] *Department of Anatomy, College of Basic Medical Sciences, Dalian Medical University, Dalian 116044, China*
[e] *Institute of Hematology, the Second Hospital of Dalian Medical University, Dalian 116027, China*
[f] *Carlson School of Chemistry and Biochemistry, Clark University, Worcester, MA 01610, USA*

GRAPHICAL ABSTRACT

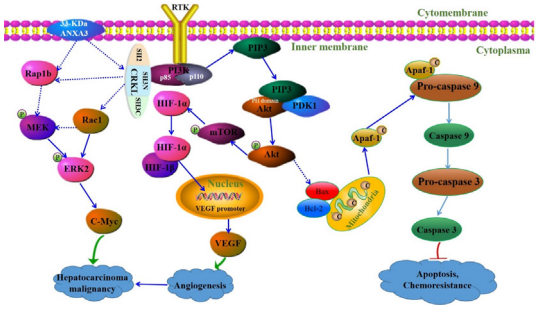

ARTICLE INFO

Article history:
Received 2 May 2020
Revised 30 October 2020
Accepted 4 November 2020
Available online 8 November 2020

Keywords:
Hepatocarcinoma
33-kDa ANXA3
Tumorigenesis

ABSTRACT

Introduction: As a member of annexin family proteins, annexin A3 (ANXA3) has 36-kDa and 33-kDa isoforms. ANXA3 plays crucial roles in the tumorigenesis, aggressiveness and drug-resistance of cancers. However, previous studies mainly focused on the role of total ANXA3 in cancers without distinguishing the distinction between the two isoforms, the role of 33-kDa ANXA3 in cancer remains unclear.
Objectives: Current work aimed to investigate the function and regulation mechanism of 33-kDa ANXA3 in hepatocarcinoma.
Methods: The expressions of ANXA3, CRKL, Rac1, c-Myc and pAkt were analyzed in hepatocarcinoma specimens by Western blotting. The biological function of 33-kDa ANXA3 in the growth, metastasis, apoptosis, angiogenesis, chemoresistance of hepatocarcinoma cells with the underlying molecular mechanism were investigated using gain-of-function strategy *in vitro* or *in vivo*.

Peer review under responsibility of Cairo University.

Production and hosting by Elsevier

* Corresponding authors at: Department of Biochemistry, College of Basic Medical Sciences, Dalian Medical University, 9 West Section, Lvshun Southern Road, Dalian, Liaoning 116044, China (S.Q. Liu). Department of Biotechnology, College of Basic Medical Sciences, Dalian Medical University, 9 West Section, Lvshun Southern Road, Dalian, Liaoning 116044, China (M.Z. Sun).
E-mail addresses: lsqsmz@163.com (S. Liu), smzlsq@163.com (M.-Z. Sun).
[1] These authors contributed equally.

https://doi.org/10.1016/j.jare.2020.11.003

Angiogenesis
Chemoresistance

Results: 33-kDa ANXA3 was remarkably upregulated in tumor tissues compared with corresponding normal liver tissues of hepatocarcinoma patients. Its stable knockdown decreased the *in vivo* tumor growing velocity and malignancy of hepatocarcinoma HepG2 cells transplanted in nude mice. The *in vitro* experimental results indicated 33-kDa ANXA3 knockdown suppressed the proliferation, colony forming, migration and invasion abilities of HepG2 cells through downregulating CRKL, Rap1b, Rac1, pMEK, pERK2 and c-Myc in ERK pathway; inhibited angiogenesisability of HepG2 cells through inactivating PI3K/Akt-HIF pathway; induced apoptosis and enhanced chemoresistance of HepG2 cells through increasing Bax/decreasing Bcl-2 expressions and inactivating caspase 9/caspase 3 in intrinsic apoptosis pathway. Accordingly, CRKL, Rac1, c-Myc and pAkt were also upregulated in hepatocarcinoma patients' tumor tissues compared with corresponding normal liver tissues.

Conclusions: The overexpression of 33-kDa ANXA3 is involved in the clinical progression of hepatocarcinoma and in the malignancy, angiogenesis and apoptosis of hepatocarcinoma cells. It is of potential use in hepatocarcinoma diagnosis and treatment.

Introduction

Hepatocarcinoma is one of the most common fatal malignant cancer, its morbidity and mortality rates are among the highest worldwide [1]. Marked progress in hepatocarcinoma treatment has been achieved in the combination of surgical resection and chemotherapy [2]. However, the relative higher metastasis, recurrence and chemoresistance of hepatocarcinoma still predict poorer prognosis of patients [3]. Therefore, improvement in the diagnosis and treatment of hepatocarcinoma depends on boost our understanding of the molecular mechanisms controlling the development, progression and aggressiveness of hepatocarcinoma. Potential indicators for the progression and drug-tolerance of hepatocarcinoma benefit better diagnosis and treatment of the patients.

Annexins are polygene superfamily of phospholipid-dependent membrane-binding and Ca^{2+}-regulated proteins [4]. The annexin are grouped into five groups: A, B, C, D, E. The groups B, C, D, E are distributed in invertebrates, fungi and moulds, plants, protists. The group A existed in vertebrates (mammalian) which has 12 members (annexin A1-11 and A13) [5,6]. The annexin A have a bipartite structure containing a conserved C-terminal annexin repeat and a variable N-terminal region. The conserved and highly α-helical annexin C-terminal core is consisted of either four or eight annexin repeats. Each annexin repeat is comprised of ~70 amino acid (AA) residues containing the Ca^{2+}- and phospholipid-binding sites [7]. The variable N-terminal domain is consisted of 20–200 AA residues leading to the diversity of functions and biological activities of annexins [8,9]. The annexin A are important in endocytosis, exocytosis, anti-coagulation, anti-inflammation and cell growth, metastasis [10–12]. Their deregulations and relocalizations participate in the incidence and malignant progression of a variety of cancers as promising carcinogenic indicators [10,13–21].

Annexin A3 (ANXA3) also called as placental anticoagulant protein3 (PAP-III) and lipocortin3, is on 4q13-q22 [10]. It has two splicing forms, 36-kDa with 323 AA and 33-kDa with 284 AA. A 39-AA-segment at the N-terminus of 36-kDa ANXA3 form is lacking in the 33-kDa form [22,23], as their nucleotide and AA sequences showed in Fig. 1. The C-terminus of ANXA3 is arranged in a cyclic array by four conserved 'annexin repeat' domains, each domain comprising five a-helices [24,25]. The ANXA3 N-terminal region with its tryptophan 5 (W5) residue involved in regulation of membrane binding and nonspecific cationic permeability. The N-terminal loss or W5 mutation in 33-kDa ANXA3 modified its interaction with membrane with increased cellular Ca^{2+}-influx [26]. ANXA3 plays important roles in vesicle trafficking, anticoagulation, liver regeneration, ion channel regulation, cell proliferation, apoptosis and metastasis [27–31]. The dysregulation of total ANXA3 (36-kDa and 33-kDa) is involved in the occurrence, development, progression, metastasis and chemoresistance of various kinds of cancers [32–42]. ANXA3 was reported as a promising biomarker candidate for diagnosis, therapy and prognosis of cancers. However, the previous studies focused on the effects of total ANXA3 on cancers. No study was attempted to distinguish between 36-kDa ANXA3 and 33-kDa ANXA3 by pinpointing the individual contribution from them in cancer development and progression. 36-kDa and 33-kDa ANXA3 might play specific roles in neutrophils and monocytes [22]. 36-kDa ANXA3 was mainly present in monocytes and 33-kDa ANXA3 in neutrophils. The undifferentiated-HL60 cells expressed both proteins, while along their differentiations, interestingly, once 33-kDa ANXA3 expression accumulated, the expression of 36-kDa ANXA3 decreased, vice versa. 33-kDa ANXA3 was upregulated in damaged rat brain area following cerebral ischemia due to the inflammatory phagocytic infiltration, while 36-kDa ANXA3 was constantly expressed rather weak and unchanged in responding to cortical tissue injury [41]. 36-kDa ANXA3 was downregulated while 33-kDa ANXA3 was upregulated in renal cell carcinoma (RCC) primary cell cultures comparing with renal cortex cell cultures [23]. These indicated that 33-kDa ANXA3 and 36-kDa ANXA3 may play different roles in biological processes.

The exact role of 33-kDa ANXA3 in cancer malignancy has not been reported. Current study is the first report on the detailed role and molecular regulation mechanism of 33-kDa ANXA3 in hepatocarcinoma even in related cancers with its presence. 33-kDa ANXA3 was linked to hepatocarcinoma carcinogenesis. 33-kDa ANXA3 was overexpressed in hepatocarcinoma patients' tumorous tissues compared to paracancerous normal liver tissues. *In vitro* experiments showed the stable knockdown of 33-kDa ANXA3 suppressed the proliferation, colony forming, migration, invasion and angiogenesis capacities, and enhanced the apoptosis, resistance to cisplatin and 5-FU of HepG2 cells. *In vivo* experiments indicated 33-kDa ANXA3 knockdown reduced tumour growth and malignancy of HepG2 cells implanted in nude mice. Mechanistic investigations revealed 33-kDa ANXA3 mediated hepatocarcinoma cell malignant behaviours, angiogenesis and chemoresistances through ERK, PI3K/Akt-HIF and intrinsic apoptotic pathways. 33-kDa ANXA3 is a potential new progression indicator and therapeutic target for hepatocarcinoma.

Materials and methods

Hepatocarcinoma patients and tissue samples

31 pairs of hepatocarcinoma patients' tumorous tissues and corresponding paracancerous normal liver tissues were provided by the Second Affiliated Hospital of Dalian Medical University,

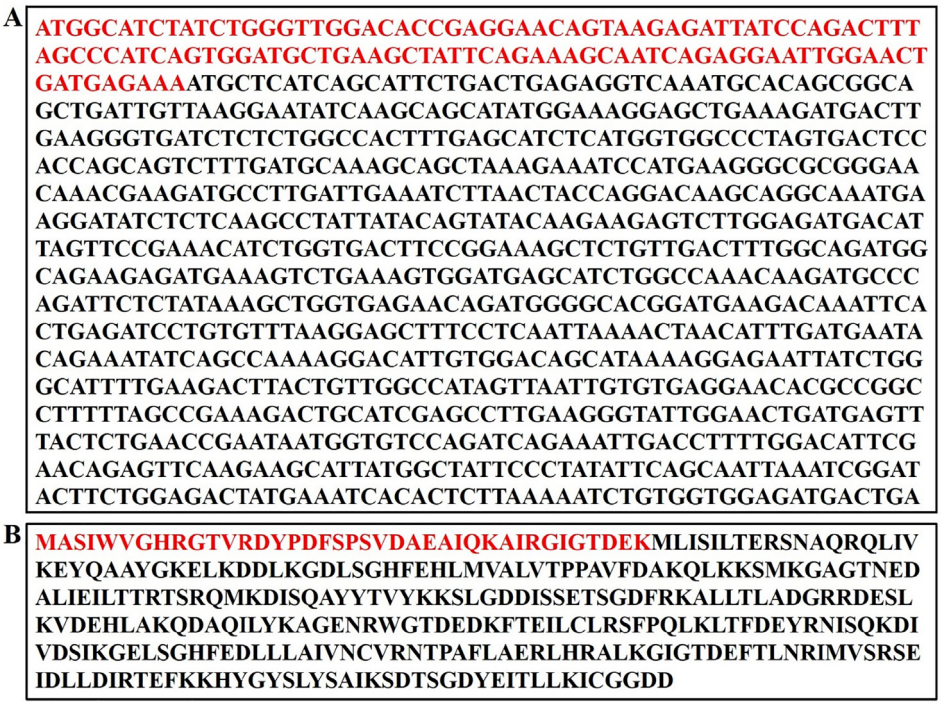

Fig. 1. Nucleotide and AA sequences of ANXA3. 36-kDa and 33-kDa *ANXA3* mRNAs encompass 972 and 855 nucleotide residues (**A**), and encode proteins composed with 323 and 284 AA residues (**B**), respectively. The sequences in red are nucleotide (**A**) and AA (**B**) residues present in 36-kDa ANXA3 while absent in 33-kDa ANXA3.

Dalian, China. Tissue specimens were immediately frozen in liquid nitrogen and stored at −80 °C. The patients included 19 males and 12 females, 12 patients ≥ 60 years and 19 patients < 60 years; 8, 3, 8 patients are cataloged into T1, T2 and T3/T4 stages, and 12 patients unknown; 14 patients are primary and 17 patients unknown; 9 patient exhibits perineuronal invasion, 17 patients no perineuronal invasion and 5 patients unknown; 9 patients have satellite nodules, 5 patients without satellite nodules and 17 patients unknown; 8 patients are HBV (hepatitis B virus) positive, 6 patients are HBV negative and 17 patients unknown; 3 patients of AFP (alpha fetoprotein) ≤ 20 IU/ml, 5 patients of 20 < AFP ≤ 400 IU/ml, 4 patients of AFP > 400 IU/ml and 19 patients unknown. Each patient signed the informed consent, tissue use and research protocol were authorized by the Ethical Committee of Dalian Medical University. All experiment protocols were carried out in accordance with the guidelines.

Cell culture

Hepatocarcinoma HepG2 and umbilical vein endothelial HUVEC cell lines were purchased from Shanghai Culture Collection of Chinese Academy of Sciences. HepG2 cell incubated in 85% RPMI-1640 (Gibco, USA) containing 15% fetal bovine serum (FBS, TransGen, China), supplement with 100 U/ml penicillin/streptomycin (Gibco, USA) at 37 °C with 5% CO_2 in a humidified incubator. HUVEC cell incubated in 90% endothelial cell medium (ECM, Science cell, USA) containing 10% FBS, 1% ECGS at 37 °C with 5% CO_2. The HUVEC cells used in this study were from passages 3 to 5.

The construction of monoclonal HepG2 cell line with stable 33-kDa ANXA3 knockdown

Three specific shRNAs (shANXA3-1: 5′-GCCTATTATACAGTA TACA-3′; shANXA3-2: 5′-GACATT AGTTCCGAAACAT-3′; shANXA3-3: 5′-GCATTATGGCTATTCCCTA-3′) to *ANXA3* (Genbank: NM_005139) were designed using Invitrogen, siDirect and Whitehead softwares. A non-targeting shRNA with 5′-GTTCTCCGAACGT GTCACGT-3′ as negative control (NC). The shRNA and shNC were constructed into pGPU6/GFP/Neo vector, named as pGPU6/GFP/Neo-shANXA3-1, pGPU6/GFP/Neo-shANXA3-2, pGPU6/GFP/Neo-shANXA3-3 and pGPU6/GFP/Neo-shNC.

4×10^5 HepG2 cells in 2 ml 85% RPMI-1640 were inoculated into one plate well, cultured for 24 h and transfected with pGPU6/GFP/Neo-shANXA3-1, pGPU6/GFP/Neo-shANXA3-2 or pGPU6/GFP/Neo-shANXA3-3 and pGPU6/GFP/Neo-shNC recombinant plasmids using lipofectamine™ 2000 (Invitrogen, USA). pGPU6/GFP/Neo-shANXA3 and pGPU6/GFP/Neo-shNC recombinant plasmids were stably transfected into HepG2 cells and screened by G418 (400 μg/ml, Invitrogen, USA) for 28 d using limited dilution screening. shANXA3-1 exhibited the most interference efficient for ANXA3, then, the monoclonal shANXA3-HepG2 cells were obtained from shANXA3-1.

Protein extraction and western blotting (WB) assay

For protein extraction from tissue specimen, about 40 mg of hepatocarcinoma tumorous tissues or corresponding non-tumor liver tissues were washed with PBS at 4 °C, then chipped out small pieces, ground into powder under liquid nitrogen and suspended with 500 μl RIPA buffer with 1 mM Na_3VO_4, 1 μg/ml leupeptin and 0.5 mM PMSF, then lysed on ice for 30 min. For protein extraction from HepG2 cells, cell pellet was collected from a 6-well plate and suspended with 50 μl RIPA buffer with 1 mM Na_3VO_4, 1 μg/ml leupeptin and 0.5 mM PMSF, and lysed on ice for 30 min. The supernatant protein was obtained by centrifugation with 12000 rpm for 30 min at 4 °C.

Equal amount protein was boiled for 5 min and separated by 10% SDS-PAGE. The target protein bands were transferred onto nitrocellulose membrane (PALL, USA), then blocked with 5% skim

milk and incubated with primary conjugated antibodies. The primary antibodies including ANXA3 (1:800, Proteintech, USA), Rap1b (1:300, Proteintech, USA), Rac1 (1:500, Proteintech, USA), CRKL (1:1000, Santa Cruz Biotechnology, USA), pMEK1/2 (1:800, pSer217/221, Cell Signaling, USA), pERK1/2 (1:500, pThr202/Tyr204, Cell Signaling, USA), c-Myc (1:500, Cell Signaling, USA), pAkt (1:800, pSer473, Cell Signaling, USA), HIF-1α (1:300, Proteintech, USA), Bcl-2 (1:500, Cell Signaling, USA), Bax (1:500, Cell Signaling, USA), Caspase 9 (1:1000, Cell Signaling, USA), Caspase 3 (1:1000, Cell Signaling, USA), GAPDH (1:5000, Proteintech, USA), ACTB (1:5000, Proteintech, USA), α-tubulin (1:5000, Proteintech, USA). Then the nitrocellulose membrane was incubated with the secondary conjugated antibody for 4 h at room temperature (RT) and washed with TBST. The target protein bands were imaged by ECL (Advansta, USA), analyzed and quantified by Bio-Rad Chemi-Doc™ MP system (Bio-Rad, USA).

Cell proliferation assay

The effect of 33-kDa ANXA3 knockdown on proliferation ability of HepG2 cell was measured by MTT. Each group 1.5×10^3 cells/well were seeded into the separate wells of a 96-well plate in 100 μl 85% RPMI-1640, incubated in humidified incubator at 37 °C, 5% CO_2 for 24, 48, 72, 96 and 120 h, then incubated with 5 mg/ml MTT at 37 °C with 5% CO_2 for 4 h in darkness. The MTT was replaced by 150 μl dimethyl sulfoxide (DMSO). The absorbances were measured by a microplate reader (Thermo, USA) at 492 nm.

33-kDa ANXA3 knockdown on HepG2 cell resistances to cisplatin and 5-fluorouracil (5-FU) were also measured by MTT. Each group 5×10^3 cells/well in 100 μl 85% RPMI-1640 were seeded into a 96-well plate, incubated in humidified incubator with 5% CO_2 at 37 °C overnight, then treated with 0, 0.25, 0.5, 1.0, 2.0, 4.0, 8.0 μg/ml cisplatin for 24 h, or treated with 0, 0.1, 0.3, 1.3, 6.5, 32.5, 162.6 μg/ml 5-FU for 48 h. The rest steps were the same as above.

Colony forming capacity assay

The influence of 33-kDa ANXA3 knockdown on HepG2 growth was also determined by colony forming assay. 1000 cells from each group in 2 ml 85% RPMI-1640 were inoculated into 6-well plate, cultured in humidified incubator at 37 °C with 5% CO_2 for 10 d until colonies were apparently visible. The cell colonies fixed with methanol for 40 min and stained with 0.5% crystal violet for 1 h. The cell colonies were observed and taken photograph by an upright light microscope (Olympus, Japan) with 100× magnification.

Cell migration and invasion assays

For migration assay, 1×10^4 cells from each group were loaded into the upper chamber of transwell unit (Corning, USA). For invasion assay, each filter insert was coated with ECM gel (Sigma, USA) for 1 h at 37 °C. 8×10^3 cells were loaded into the upper compartment of transwell unit. Then, each chamber was mounted onto a 24-well plate containing 600 μl 20% FBS in 80% RPMI-1640 and cultured in humidified incubator at 37 °C with 5% CO_2 for 48 h. The migrated or invaded cells at the insert's lower surface were fixed with methanol, stained with 0.5% crystal violet and taken photograph by microscope with 100× magnification.

Wound-healing assay

The influence of 33-kDa ANXA3 knockdown on the motility of HepG2 cells was measured by *in vitro* wound-healing assay. 100 μl 85% RPMI-1640 with 5×10^5 cells from each group were loaded into a 6-well plate and incubated in humidified incubator with 5% CO_2 at 37 °C for 24 h. The cell layer was scratched with a sterile pipet tip and washed with PBS, then incubated at 37 °C for 48 h. The cell cultures were then immediately imaged for analyzing the rate of gap closure at 0 and 24 h under a microscope (Olympus, Japan) with 100× magnification.

F-actin cytoskeleton staining assay

FITC-phalloidin staining assay was used to check the effect of 33-kDa ANXA3 knockdown on HepG2 cytoskeleton structure. The glass slides (ϕ25mm, 0.17 mm thick) were placed into 6-well plates and covered with 4500 cells from each group in 100 μl 85% RPMI-1640 with 5% CO_2 at 37 °C for 24 h. Then the slides were fixed with 4% paraformaldehyde for 15 min and washed with PBS, dehydrated in pre-cooled acetone (−20 °C) and incubated with 200 μl 400 nM FITC-Phalloidin with 1% BSA. Following PBS washing for 3 times, the cells were counterstained with 100 μl 50 nM Hoechst 33258 for 3 min in darkness, then imaged for actin cytoskeleton organization and filament arrangement by randomly selecting five visual fields using a laser confocal microscope (Leica, Tes-sp5, Germany) with 1000×.

Enzyme-linked immunosorbent assay (ELISA)

To determine the VEGF protein expression level, we obtained tumor-conditioned medium (TCM) from scramble-HepG2 and shANXA3-HepG2 cells which were incubated in serum-free RPMI-1640 medium with 5% CO_2 at 37 °C for 24 h. The amount of VEGF protein in the TCM from the scramble-HepG2 and shANXA3-HepG2 cells was determined by ELISA kit (Proteintech, USA) according to the manufacturer's instructions.

HUVEC cell tube formation assay

33-kDa ANXA3 knockdown on angiogenesis capacity of HepG2 cells was measured using HUVEC cell tube formation assay. 2 ml 85% RPMI-1640 with 2×10^5 cells from scramble-HepG2 and shANXA3-HepG2 groups were inoculated into the 6-well plates, incubated in humidified incubator at 37 °C with 5% CO_2 for 24 h, then the medium was replaced by serum-free RPMI-1640 medium, incubated in humidified incubator at 37 °C with 5% CO_2 for 24 h and centrifuged with 1000 rpm for 10 min to collect supernatants as TCM. Simultaneously, each well of a 24-well plate was coated with 250 μl 10 mg/ml matrigel (Corning, USA) and maintained at 37 °C for 1 h. Then 1×10^5 HUVEC cells in 200 μl serum-free ECM basal medium mixed with 200 μl TCM were loaded to each well coated with matrigel, incubated in humidified incubator with 5% CO_2 at 37 °C for 6 h, the tube formation of different group cells were photographed using an inverted (Olympus, Japan) with 100×, tube formation amount and capillary length were quantified with Angiogenesis Analyzer of Image J software (National Institutes of Health, Bethesda, MD, USA).

Cell apoptosis assay

The influence of 33-kDa ANXA3 silencing on HepG2 cell apoptosis was measured by flow cytometry method. The cell pellets from each group were harvested, collected and dissolved in 500 μl binding buffer, incubated with 5 μl Annexin Ⅴ-FITC and 5 μl PI in darkness for 30 min at RT and immediately subjected to flow cytometry analysis.

Cisplatin-induced HepG2 apoptosis following 33-kDa ANXA3 knockdown was measured by flow cytometry. Each group 1×10^6 cells/well in 100 μl 85% RPMI-1640 were seeded into a 6-well plate, incubated with 5% CO_2 at 37 °C overnight, then trea-

ted with 2 μg/ml cisplatin and incubated in humidified incubator at 37 °C with 5% CO_2 for 24 h. The rest steps were the same as above.

Hoechst 33258 staining assay

The influence of 33-kDa ANXA3 silencing on cisplatin- and 5-FU-induced apoptosis of HepG2 cells were assayed by Hoechst 33258 staining method. The each group 5×10^3 cells/well were seeded into a 96-well plate in 100 μl 85% RPMI-1640, incubated in humidified incubator with 5% CO_2 at 37 °C overnight, administrated with 0, 1, 2 μg/ml cisplatin for 24 h or 0, 30, 60 μg/ml 5-FU for 48 h with 5% CO_2 at 37 °C, then washed with PBS, fixed with 4% paraformaldehyde at 4 °C for 30 min, stained with Hoechst 33258 solution in darkness for 15 min. Finally, the different group cells were immediately imaged using an inverted fluorescence microscope (Olympus, Japan) with 200×.

ANXA3 knockdown suppresses in vivo tumorigenicity of HepG2 in nude mice

Nude mice xenograft model was used to study the effect of 33-kDa ANXA3 downregulation on the *in vivo* tumorigenicity and malignancy of HepG2 cells. 2 ml 85% RPMI-1640 with 1×10^7 cells from shANXA3-HepG2 and scramble-HepG2 were subcutaneously implanted into the right flank of each BABL/c nude mouse (4–6 w, n = 5). Tumor size was measured and calculated as $V = a \times b^2/2$ in which a and b (in mm) refer to the greatest diameter and the length perpendicular to a of formed solid tumor every one week. In 80 days following tumor cell transplantations, tumorous xenografts were immediately dissected from euthanized mice, weighted, appropriately stored in prior to use. Nude BABL/c mice were offered by the specific pathogen free (SPF) Animal Laboratory Center of Dalian Medical University. Investigation was carried out according to the ethical standards of the national and international guidelines, and approved by the Experiment Animal Ethical Committee of Dalian Medical University.

Hematoxylin-eosin (HE) staining and immunohistochemistry (IHC) assays

Dissected solid tumors were fixed with 10% formalin, embedded in paraffin, cut into 4-μm slices, stained in HE solution and imaged by microscope at 400×. For IHC assays of ANXA3, Ki-67, Bcl-2 and Bax, the paraffin slices were dewaxed by xylene, rehydrated by gradient ethanol, merged in 3% H_2O_2 for 30 min, blocked with 10% non-immune goat serum, and incubated with the primary antibodies including ANXA3 (1:100, Proteintech, USA), Ki-67 (1:100, ZSGB-BIO, China), Bcl-2 (1:100, Cell Signaling, USA), Bax (1:100, Cell Signaling, USA) at 4 °C overnight. Then, the slides incubated with peroxidase-conjugated streptavidin at 37 °C for 25 min, washed with PBS and stained by DAB at RT. The slides were counterstained with hematoxylin, dehydrated by gradient ethanol and clarified by xylene, imaged by microscope (Olympus, Japan) with 200×. Brown staining refers to the positive reaction.

Data procession and statistical analysis

All data were analyzed using GraphPad Prism 5.0 (La Jolla, USA). The data was represented as mean ± SD of at least three independent experiments. The differences were analyzed by unpaired Student's *t*-test. The differences with $P \leq 0.05$ were significantly.

Results

33-kDa ANXA3 was overexpressed in hepatocarcinoma patients' tumorous tissues

The protein expression levels of ANXA3 in tumorous tissues and paired non-tumor liver tissues from 31 hepatocarcinoma patients were quantified by WB assay. As shown in Fig. 2A and B, the overall expression level of ANXA3 or both the levels of 36-Da and 33-kDa ANXA3 were apparently more frequently upregulated in patients' tumorous tissues. The protein expression levels of 33-kDa and 36-kDa ANXA3 were increased by 3.3-fold ($P = 0.0013$, Fig. 2C) and 4.8-fold ($P = 0.0014$, Fig. 2C) in tumorous tissues than paracancerous non-tumor liver tissues. These showed both 33-kDa ANXA3 and 36-kDa ANXA3 were involved in hepatocarcinoma clinical malignancy. Previous studies have focused on the total ANXA3 in cancer, neither 33-kDa ANXA3 nor 36-kDa ANXA3 was separately investigated in cancer field. Different from previous studies, current work showed both the respective overexpressions of 33-kDa ANXA3 and 36-kDa ANXA3 linked to hepatocarcinoma occurrence. Meanwhile, we analyzed the correlation of 33-kDa ANXA3 and 36-kDa ANXA3 with clinicopathologic parameters of hepatocarcinoma patients, however, the expression levels of 33-kDa ANXA3 and 36-kDa ANXA3 were not associated with age, gender, TNM stage, HBV and perineuronal invasion (unshown).

33-kDa ANXA3 knockdown suppressed growth ability of HepG2 cells

In order to reveal the function and molecular mechanism of 33-kDa ANXA3 in hepatocarcinoma, we constructed the monoclonal shANXA3-HepG2 cells with stable knockdown of 33-kDa ANXA3 using the combinations of shRNA interference, G418 screening and limited dilution method. Compared with scramble-HepG2 cells, no apparent expression level change of 36-kDa ANXA3 was detected in shANXA3-HepG2 cells, while, 33-kDa ANXA3 and total ANXA3 levels in shANXA3-HepG2 cells were decreased by 98.0 ± 2.1% ($P = 0.0002$) and 52.8 ± 0.1% ($P = 0.0016$) (Fig. 3A). Excluding the participation of 36-kDa ANXA3 expression change, our established monoclonal shANXA3-HepG2 cell line was an appropriate subject for investigating the role of 33-kDa ANXA3 in malignant properties of HepG2 cells.

33-kDa ANXA3 knockdown reduced the *in vitro* proliferation of HepG2. The transfection of pGPU6/GFP/Neo vector showed no effect on HepG2 proliferation (Fig. 3B). While, compared with scramble-HepG2 cells, 33-kDa ANXA3 stable knockdown led to the decreases of proliferative capacities of shANXA3-HepG2 cells with 16.8% ($P < 0.001$), 17.7% ($P < 0.001$), 18.6% ($P < 0.001$) and 15.7% ($P < 0.001$) at time points of 48, 72, 96 and 120 h (Fig. 3B). Its knockdown also decreased the colony forming capacity of HepG2 cells. The number of formed colonies of shANXA3-HepG2 cells was 200.0 ± 8.1 that was only ~42.1% of that of scramble-HepG2 cells (347.0 ± 13.3, $P = 0.0007$, Fig. 3C). Meanwhile, 33-kDa ANXA3 knockdown also decreased the colony size of shANXA3-HepG2 than scramble-HepG2, the colony size of shANXA3-HepG2 cells decreased by 48.1% compared with scramble-HepG2 cells ($P = 0.0024$, Fig. 3C). Its knockdown suppresses the *in vitro* growth of HepG2 cells.

33-kDa ANXA3 knockdown inhibited migration, invasion and motility abilities of HepG2 cells

The transfection of empty vector showed no influence on the *in vitro* migration, invasion (Fig. 4A) and motility (Fig. 4B) capacities, while the knockdown of 33-kDa ANXA3 clearly decreased these malignant behaviours of HepG2 cells. The migrated and

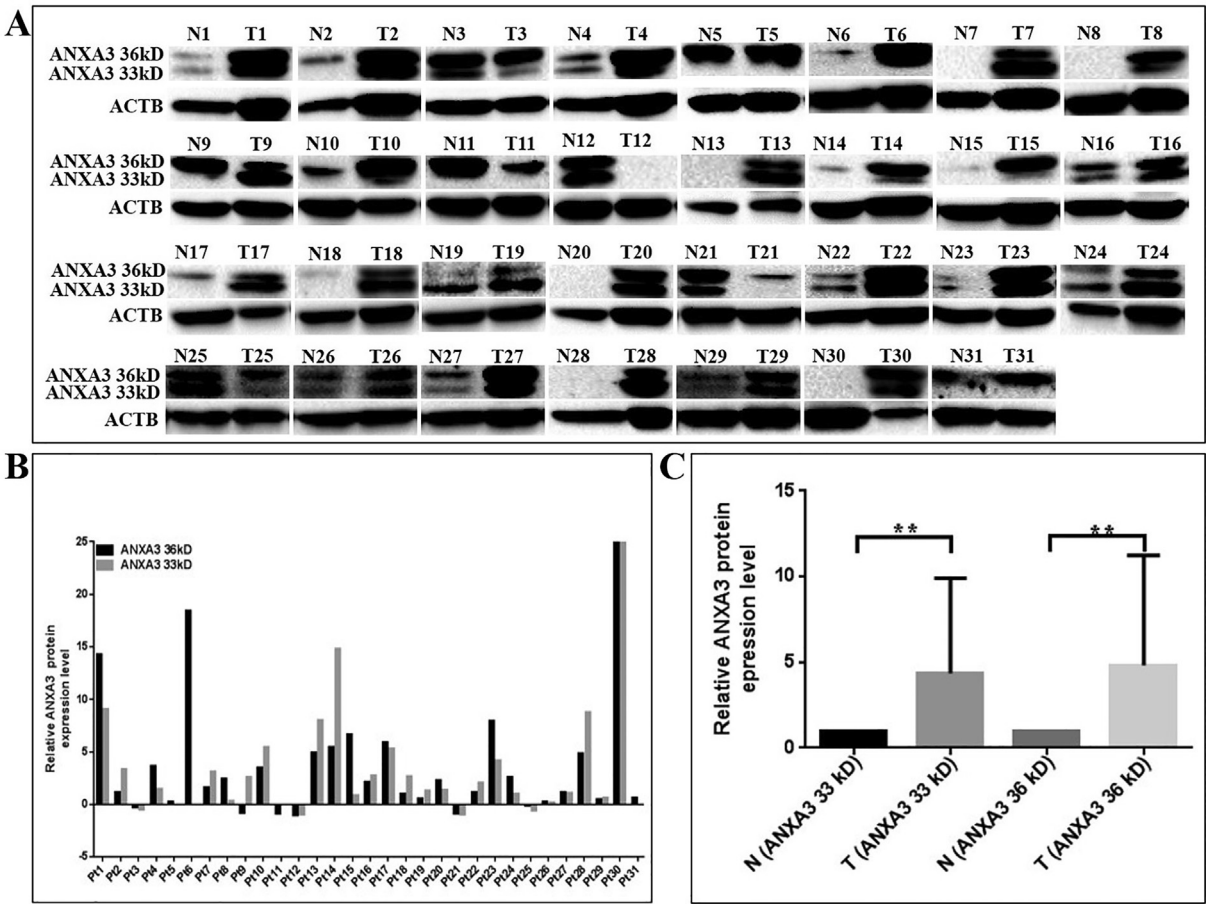

Fig. 2. ANXA3 was upregulated in hepatocarcinoma tissues. (**A**) WB assay of ANXA3 expressions in 31 pairs of tumorous and paracancerous non-tumor liver tissues from hepatocarcinoma patients. Comparative abundances (**B**) and quantified relative level fold changes (**C**) of 33-kDa and 36-kDa ANXA3 in patients' tumorous tissues than normal ones. ** refers to $P < 0.01$.

invaded numbers of shANXA3-HepG2 cells were measured as 169.0 ± 7.0 and 132.3 ± 7.2 per view that were only 55.1% ($P < 0.0001$) and 41.5% ($P = 0.0008$) of those, 376.7 ± 6.3 and 226.0 ± 7.2, of the scramble-HepG2 cells. 33-kDa ANXA3 downregulation also reduced the motility ability of HepG2 (Fig. 4A). Wound healing assay showed the migrated distance of shANXA3-HepG2 was 1.3 ± 0.28 mm that was only 37.3% ($P = 0.0132$) of that of the scramble-HepG2 cells (Fig. 4B).

Cytoskeleton are closely associated with cell movement. The change of F-actin microfilaments organization following 33-kDa ANXA3 knockdown in HepG2 was investigated by fluorescence microscopy using FITC-labeled phalloidin. As in Fig. 4C, 33-kDa ANXA3 downregulation resulted in reduced microfilaments of F-actin in shANXA3-HepG2 cells, while, no difference was observed between scramble-HepG2 and HepG2 cells. More abundant and ordered F-actin microfilaments evenly radiated to cell membrane from the cell nucleus in HepG2 and scramble-HepG2 cells, while, less abundant and disordered F-actin filaments were present in shANXA3-HepG2 cells. The decreased expression and arrangement of cytoskeleton F-actin caused by 33-kDa ANXA3 knockdown might contribute to the decreased invasion, migration and motility potentials of HepG2 cells.

33-kDa ANXA3 downregulation inhibited angiogenesis and enhanced apoptosis of HepG2 cells

VEGF is a ubiquitous and potent activator of angiogenesis, first, we detected the level of VEGF in TCM to explore whether VEGF is involved in 33-kDa ANXA3-stimutaed HUVEC cell tube formation. We found HepG2 cells could secret the VEGF to medium, and the level of VEGF in TCM obtained from shANXA3-HepG2 cells was significantly decreased by compared to scramble-HepG2 cells ($P = 0.0001$, Fig. 5A). Our results indicate the secreted VEGF may be associated with 33-kDa ANXA3-induced angiogenesis. We further detected the influence of 33-kDa ANXA3 downregulation on angiogenesis capacity of HepG2 cells was tested using HUVEC cell *in vitro* tube formation assay. 33-kDa ANXA3 knockdown resulted in the decreased formation of capillary-like structure of HUVEC cells (Fig. 5B). 33-kDa ANXA3 downregulation inhibited angiogenesis and 33-kDa ANXA3 level in HepG2 cells positively correlated with its induction on tube formation ability of HUVEC cells.

Flow cytometry assay indicated 33-kDa ANXA3 knockdown promoted the apoptosis of HepG2. The percentages of cells in early phase for shANXA3-HepG2 and scramble-HepG2 cells were determined as 19.0 ± 3.3% and 6.5 ± 1.1%. ANXA3 knockdown led to an increased early apoptotic rate of shANXA3-HepG2 by 1.9-fold than scramble-HepG2 cells (Fig. 5C, $P = 0.0188$), while, showed no influence on late apoptosis of HepG2 (Fig. 5C). 33-kDa ANXA3 knockdown potentially suppressed the viability of HepG2 cells *via* prompting their apoptosis at early phase.

33-kDa ANXA3 downregulation enhanced HepG2 cells resistance to cisplatin and 5-FU

Cisplatin and 5-FU are adjuvant drugs in clinical treatment of hepatocarcinoma patients. Total ANXA3 was reported associated

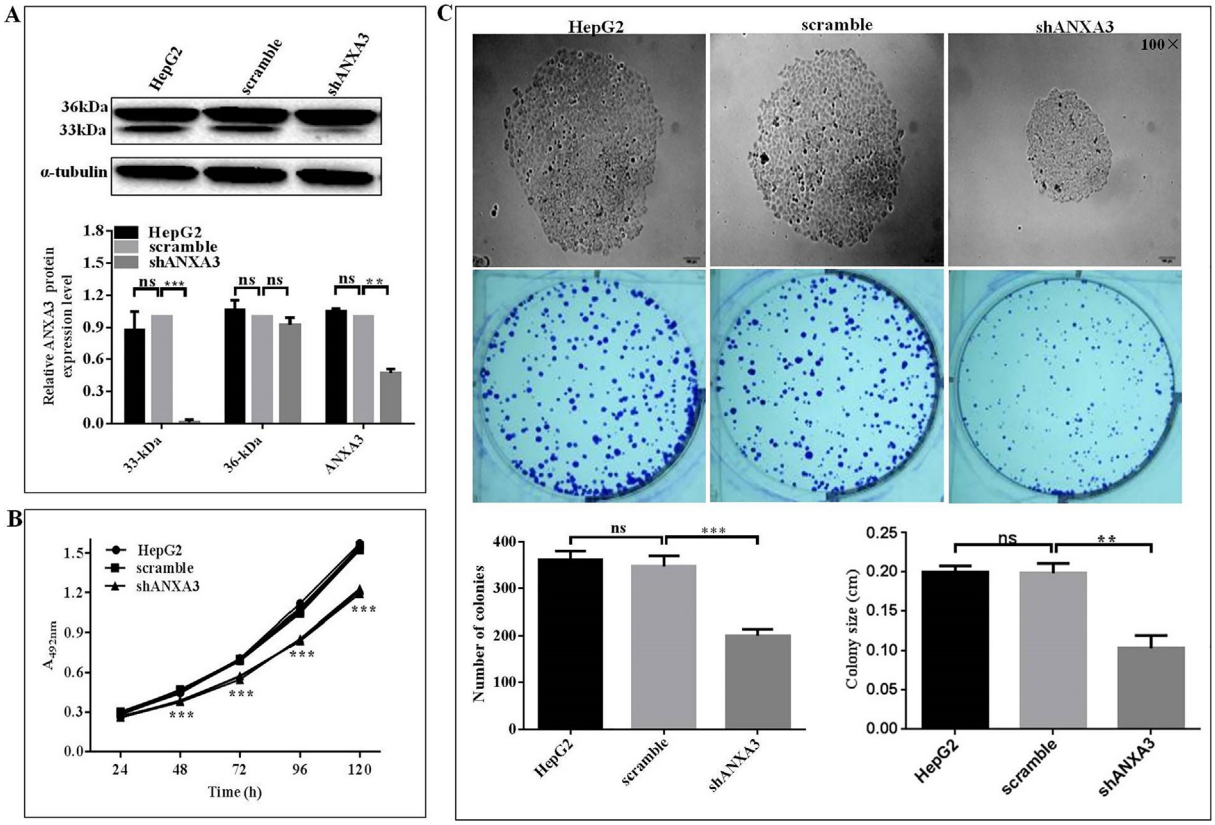

Fig. 3. 33-kDa ANXA3 knockdown suppressed *in vitro* growth of HepG2 cell. (**A**) 33-kDa ANXA3 was stably downregulated in monoclonal shRNA-HepG2 than scramble-HepG2 cells. 33-kDa ANXA3 knockdown decreased the proliferation ability (**B**) and colony forming capacity (**C**) of HepG2 cells. **, *** and ns refer to the *P* values <0.01, <0.001 and non-statistical significance.

with drug resistance of tumor [37,39], in current work, we revealed 33-kDa ANXA3 was involved in the chemosensitivities of HepG2 cells to cisplatin and 5-FU. MTT results showed that 33-kDa ANXA3 downregulation enhanced the resistances of HepG2 cells to cisplatin and 5-FU. ShANXA3-HepG2 cells showed decreased sensitivities to cisplatin ($P = 0.0114$) and 5-FU ($P = 0.0023$) than scramble cells (Fig. 6A). The IC_{50} values of cisplatin on HepG2, scramble-HepG2 and shANXA3-HepG2 cells in 24 h were 1.02 ± 0.23, 1.06 ± 0.26, 1.72 ± 0.32, and those of 5-FU on HepG2, scramble-HepG2 and shANXA3-HepG2 cells in 48 h were 3.58 ± 0.31, 3.64 ± 0.13, 6.68 ± 1.83. 33-kDa ANXA3 downregulation potentially increased the resistance of hepatocarcinoma cells to chemotherapy.

The effect of 33-kDa ANXA3 downregulation on cisplatin-induced HepG2 apoptosis was analyzed by flow cytometry analysis. Its knockdown decreased HepG2 apoptosis induced by cisplatin and 5-FU at early phase. The percentages of cells distributed in early phase for shANXA3-HepG2 and scramble-HepG2 cells with cisplatin treatments were 8.2 ± 2.0% and 21.4 ± 0.4%, the early phase apoptotic rate of shANXA3-HepG2 cells decreased by 61.7% than scramble-HepG2 cells ($P = 0.0111$, Fig. 6B). However, its knockdown showed no influence on the late apoptosis of HepG2 cells with cisplatin treatment ($P = 0.3170$, Fig. 6B). 33-kDa ANXA3 level change is of potential use as an indicator in chemotherapy of hepatocarcinoma.

The influences of 33-kDa ANXA3 knockdown on HepG2 apoptosis induced by cisplatin and 5-FU were further analyzed using Hoechst 33258 staining assay. Its downregulation weakened the sensitivities of HepG2 cells to cisplatin- (Fig. 6C) and 5-FU-induced apoptosis (Fig. 6D). The condensed and fragmented nuclei of apoptotic cells were significantly reduced in the shANXA3-HepG2 group cells than the scramble-HepG2 group cells (Fig. 6B). 33-kDa ANXA3 downregulation inhibited HepG2 cells apoptosis induced by cisplatin and 5-FU.

33-kDa ANXA3 downregulation inhibited in vivo tumorigenicity of HepG2 cells

We further investigated the influence of 33-kDa ANXA3 silencing on *in vivo* tumorigenicity of HepG2 cells using xenograft tumor model. The shANXA3-HepG2 and scramble-HepG2 cells were subcutaneously inoculated into the right flanks of nude mice. After inoculation for 80 days, the tumor sizes of shANXA3-HepG2-transplanted mice were smaller than scramble-HepG2-transpalnted mice (Fig. 7A). The primary tumor mass from shANXA3-HepG2-transplanted mice was averaged as 0.007 ± 0.004 g that was ~94.9% decreased compared with the averaged mass of 0.136 ± 0.078 g from scramble-HepG2-transplanted mice (Fig. 7A, $P = 0.0442$). 33-kDa ANXA3 knockdown suppressed the *in vivo* tumorigenicity and tumor growth of HepG2 cells.

Consistent with 33-kDa ANXA3 downregulation increasing the *in vitro* apoptosis of HepG2 cells, its knockdown also enhanced the *in vivo* tumor cell apoptosis in primary tumour induced by HepG2 transplantation. HE staining assay showed apparent necrosis and sporadically apoptotic cells appearing in the slices of primary tumors from shANXA3-HepG2-tansplanted mice, while such situations were not observed in primary tumors from scramble-HepG2 group mice (Fig. 7B).

IHC assays were further performed to measure cell proliferation marker Ki-67 and apoptosis marker Bcl-2 and Bax in

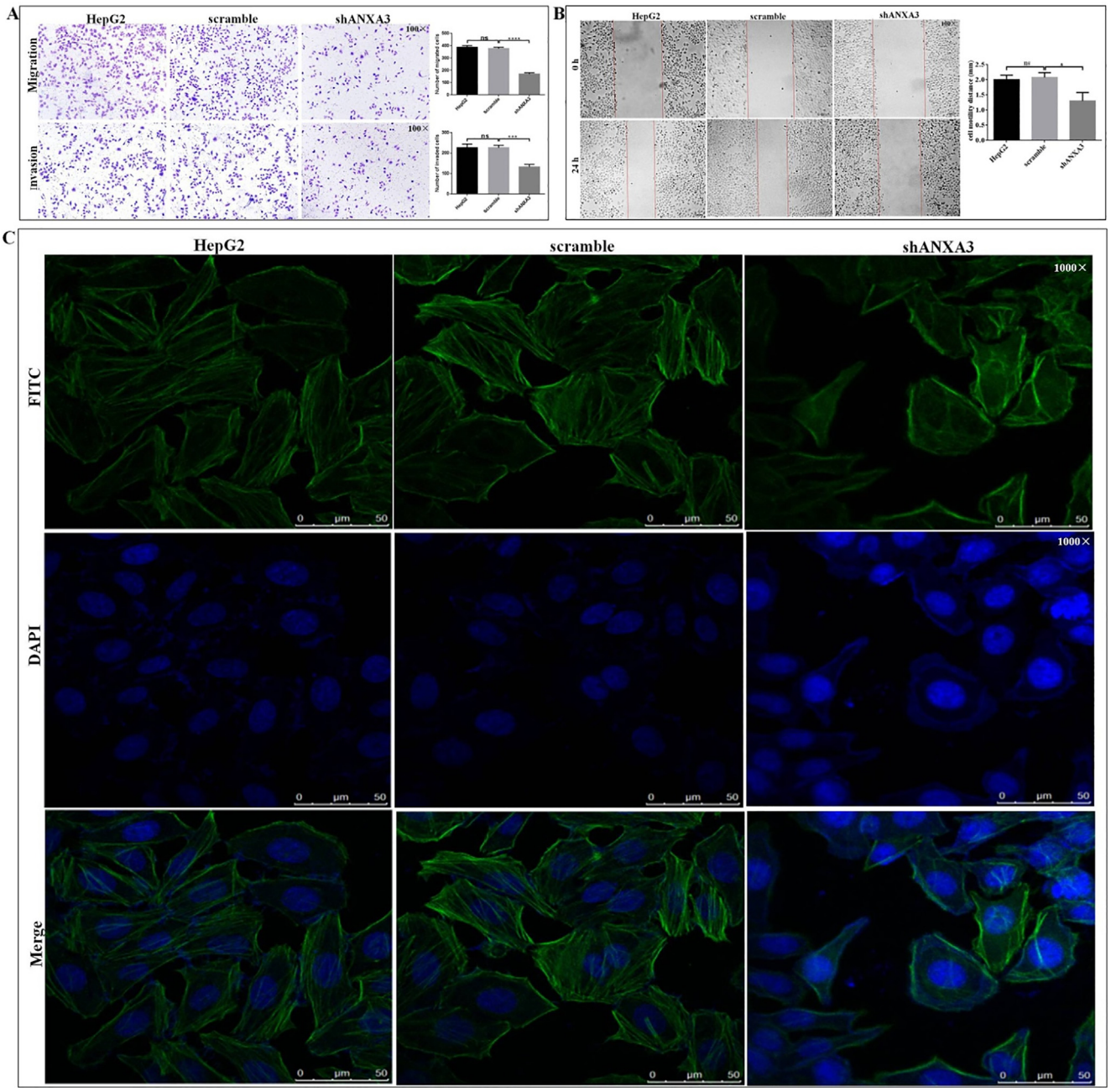

Fig. 4. 33-kDa ANXA3 knockdown (**A**) inhibited the migration, invasion and (**B**) motility capacities of HepG2 cells. (**C**) 33-kDa ANXA3 knockdown decreased the expression and distorted the filament arrangement of cytoskeleton F-actin in HepG2 cell by FITC-phalloidin assay. *, *** and **** refer to the $P < 0.05$, 0.001 and 0.0001, and ns refers to non-statistical significance.

tumorous tissues. The expression levels of Ki-67, Bcl-2 and VEGF in primary tumor from scramble-HepG2 group mice were higher than that in the shANXA3-HepG2-tansplanted mice, meanwhile, as Bax expression was lower in primary tumor from scramble-HepG2 group mice than that in the shANXA3-HepG2-tansplanted mice, 33-kDa ANXA3 downregulation resulted in a increased Bax/Bcl-2 ratio (Fig. 7C). The results further demonstrated 33-kDa ANXA3 downregulation suppressed the growth, angiogenesis and promoted apoptosis of hepatocarcinoma cells *in vivo*, its downregulation inhibited the *in vivo* tumorigenicity of hepatocarcinoma cells *via* inhibiting their proliferation, angiogenesis and promoting their apoptosis.

33-kDa ANXA3 downregulation inhibited tumorigenesis, angiogenesis and increased chemoresistance of HepG2 cells via inhibiting ERK, PI3K/Akt-HIF and intrinsic apoptotic pathways

The underlying molecular regulation mechanism of 33-kDa ANXA3 in hepatocarcinoma is unknown. We measured the expression levels of ERK pathway-related molecules. The stable knockdown of 33-kDa ANXA3 resulted in the protein expression levels of Rap1b, Rac1, CRKL, pMEK, pERK2 and c-Myc decreased by 47.7% ($P = 0.0451$), 37.2% ($P = 0.0145$), 36.3% ($P = 0.0047$), 42.9% ($P = 0.0422$), 43.2% ($P = 0.0269$) and 41.8% ($P = 0.0046$) in shANXA3-HepG2 cells compared to the scramble group cells (Fig. 8A). ERK pathway acts important roles in the growth and

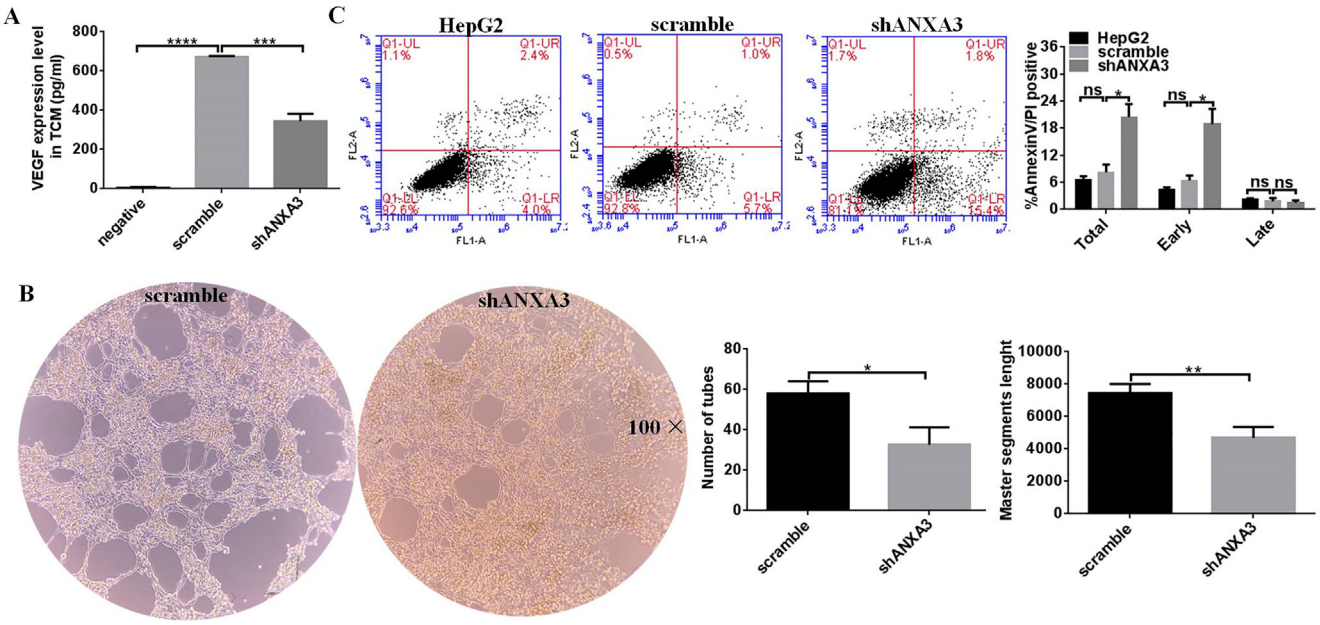

Fig. 5. 33-kDa ANXA3 knockdown inhibited the *in vitro* angiogenesis and enhanced apoptosis of HepG2 cell. (**A**) 33-kDa ANXA3 knockdown inhibited the secretion of VEGF in TCM. shRNA-HepG2 than scramble-HepG2 cells were incubated in serum-free RPMI-1640 for 24 h and TCM was collected. The level of VEGF in TCM was measured by ELISA, 85% RPMI-1640 with 15% FBS as negative control. (**B**) 33-kDa ANXA3 knockdown inhibited the tube formation ability of HUVEC induced by HepG2 cells. (**C**) 33-kDa ANXA3 knockdown promoted HepG2 cells apoptosis. *, **, *** and **** refer to the $P < 0.05$, <0.01, <0.001, <0.0001 and ns refers to no statistical difference.

metastasis of tumor cells. We showed that 33-kDa ANXA3 downregulation might suppress the growth, migration and invasion abilities of HepG2 cells *via* deactivating ERK pathway.

This work linked PI3K/AKT and Bax/Bcl-2 signal transductions in 33-kDa ANXA3-mediated angiogenesis and apoptosis of hepatocarcinoma cells. The protein expression levels of pAkt and HIF-1α were decreased by 31.1% ($P = 0.0427$) and 38.2% ($P = 0.0428$) in shANXA3-HepG2 cells compared with scramble-HepG2 cells (Fig. 8B). Meanwhile, 33-kDa ANXA3 knockdown decreased Bcl-2 expression by 30.6% ($P = 0.0403$) and increased Bax expression by 39.8% (Fig. 8B, $P = 0.0291$) in HepG2 cells, which lead to Bax/Bcl-2 expression ratio increased by 101.6% (Fig. 8B, $P < 0.005$). 33-kDa ANXA3 downregulation potentially inhibited the angiogenesis and promoted apoptosis of HepG2 cells *via* deactivating PI3K/Akt and Bcl-2/Bax pathways.

33-kDa ANXA3 downregulation enhanced HepG2 cells resistances to cisplatin and 5-FU (Fig. 6). We then investigated the potential molecular regulation mechanisms. WB results showed the levels of pAkt and Bcl-2 were increased by ~30.6% ($P = 0.0361$) and ~34.0% ($P = 0.0101$) in cisplatin treated-shANXA3-HepG2 cells compared with cisplatin treated-scramble-HepG2 cells, while, Bax expression level was decreased by ~ 56.1% ($P = 0.0411$) (Fig. 8C). The activities of caspase 9 and caspase 3 in cisplatin-induced apoptosis of HepG2 cells were measured. The cleavage forms of caspase 9 and caspase 3 appeared in HepG2 with the exposure to cisplatin. The levels of cleaved- caspase
9 and -caspase 3 were decreased by ~35.5% ($P = 0.0001$) and ~36.4% ($P = 0.0086$) in cisplatin treated-shANXA3-HepG2 cells than cisplatin treated-scramble-HepG2 cells (Fig. 8C). No cleavage forms of caspase 9 and caspase 3 appeared in HepG2 cells without exposure to cisplatin, and no apparent expression changes were observed for pro-caspase 9 ($P = 0.8081$) and pro-caspase 3 ($P = 0.1351$, Fig. 8C). 33-kDa ANXA3 knockdown increased HepG2 cells resistance to cisplatin through suppressing the intrinsic apoptotic pathway.

Expression patterns of key molecules in ERK and PI3K/Akt pathways in tumorous tissues of hepatocarcinoma

WB assay showed the levels of CRKL, Rac1, c-Myc and pAkt were increased by 61.5% ($P = 0.0004$, Fig. 9A), 76.5% ($P = 0.015$, Fig. 9B), 56.9% ($P = 0.0036$, Fig. 9C) and 31.6% ($P = 0.0482$, Fig. 9D) in 31 pairs of hepatocarcinoma patients' tumorous tissues and paracancerous normal liver tissues. As already mentioned above the levels of CRKL, Rac1, c-Myc and pAkt were accordingly decreased in HepG2 cells following 33-kDa ANXA3 knockdown (Fig. 8), it is clear that 33-kDa ANXA3 probably enhances the malignant behaviours and chemo-sensitivities of hepatocarcinoma cells and clinical progression of hepatocarcinoma patients *via* ERK, PI3K/Akt and intrinsic apoptotic pathways.

Discussion

ANXA3, a membrane related protein predominantly expressing in cytoplasm, is abnormally expressed in various cancers. Its deregulation is related with the development, occurrence, progression and drug resistance of cancer. ANXA3 might specifically functionalize either as a tumor suppressor or tumor promoter depending on the types or sub-types of different cancers [27]. It is even reported as an underlying biomarker for the diagnosis, therapy and prognosis of certain cancers. ANXA3 has 36-kDa and 33-kDa isoforms [22]. Most studies reported a single protein band in the WB image and without distinguishing them. So, the majority of studies focused on the role of total ANXA3 in cancers, unfortunately, they did not pinpoint the exact role of the individual ANXA3 subtype in cancer development and malignancy. Until now the expression patterns of 36-kDa and 33-kDa ANXA3 have been only documented in human monocytes and neutrophils [22], in rat brain [41] and in RCC [23]. However, the exact role of 33-kDa ANXA3 in cancer remains unknown. The better understanding on the functional action and molecular mechanism of ANXA3 isoforms

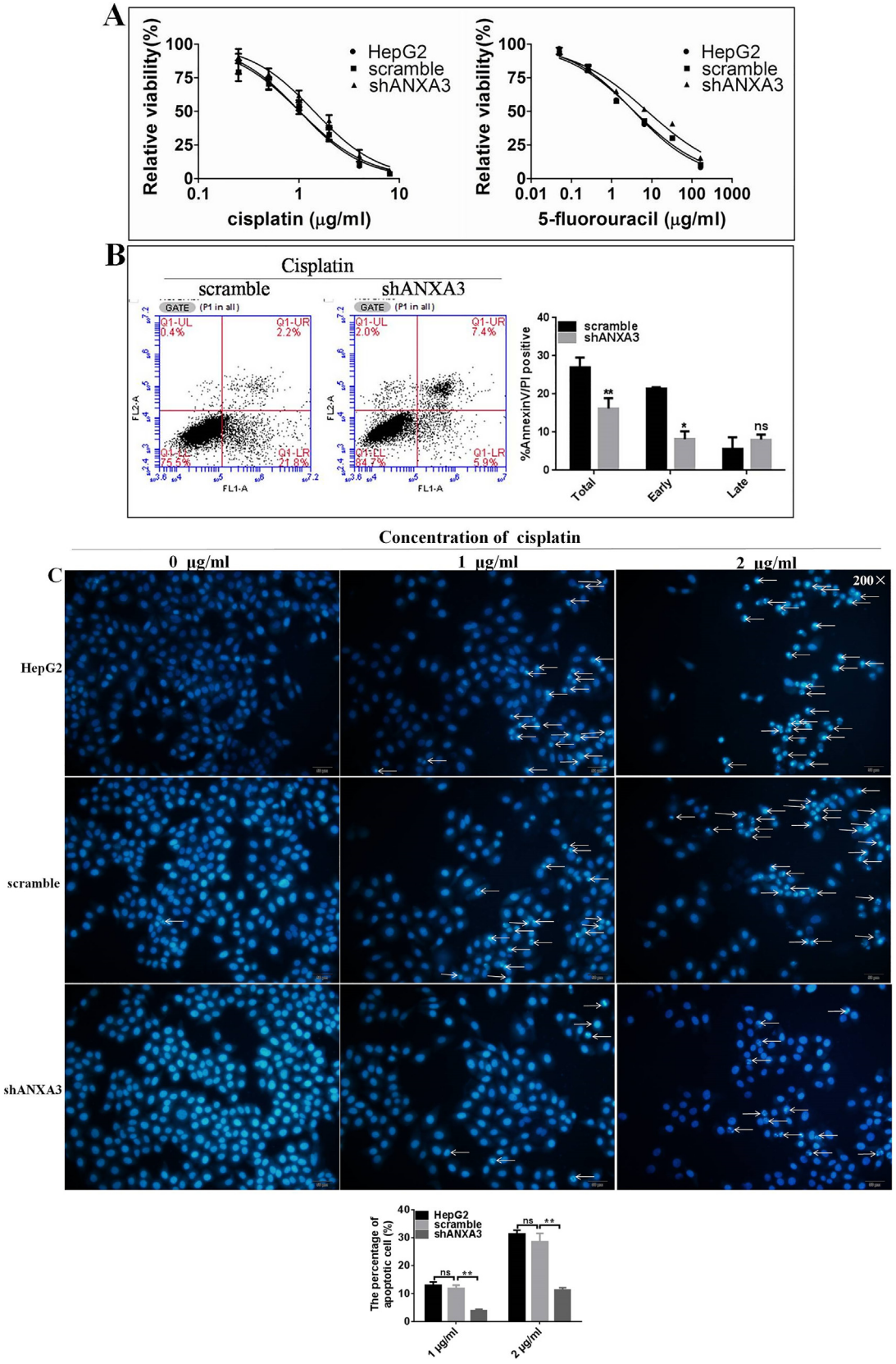

Fig. 6. 33-kDa ANXA3 knockdown enhanced HepG2 cell resistances to cisplatin and 5-FU. (**A**) 33-kDa ANXA3 knockdown enhanced HepG2 resistances to cisplatin and 5-FU by MTT assay. (**B**) 33-kDa ANXA3 knockdown inhibited cisplatin-induced HepG2 apoptosis by flow cytometry assay. (**C, D**) 33-kDa ANXA3 knockdown reduced the sensitivities of HepG2 to cisplatin- and 5-FU-induced apoptosis by Hoechst 33258 staining assay. * and ** refer to $P < 0.05$ and 0.01, ns refers to no statistical difference. Arrows marked the apoptotic cells for representing nuclear condensation/fragmentation.

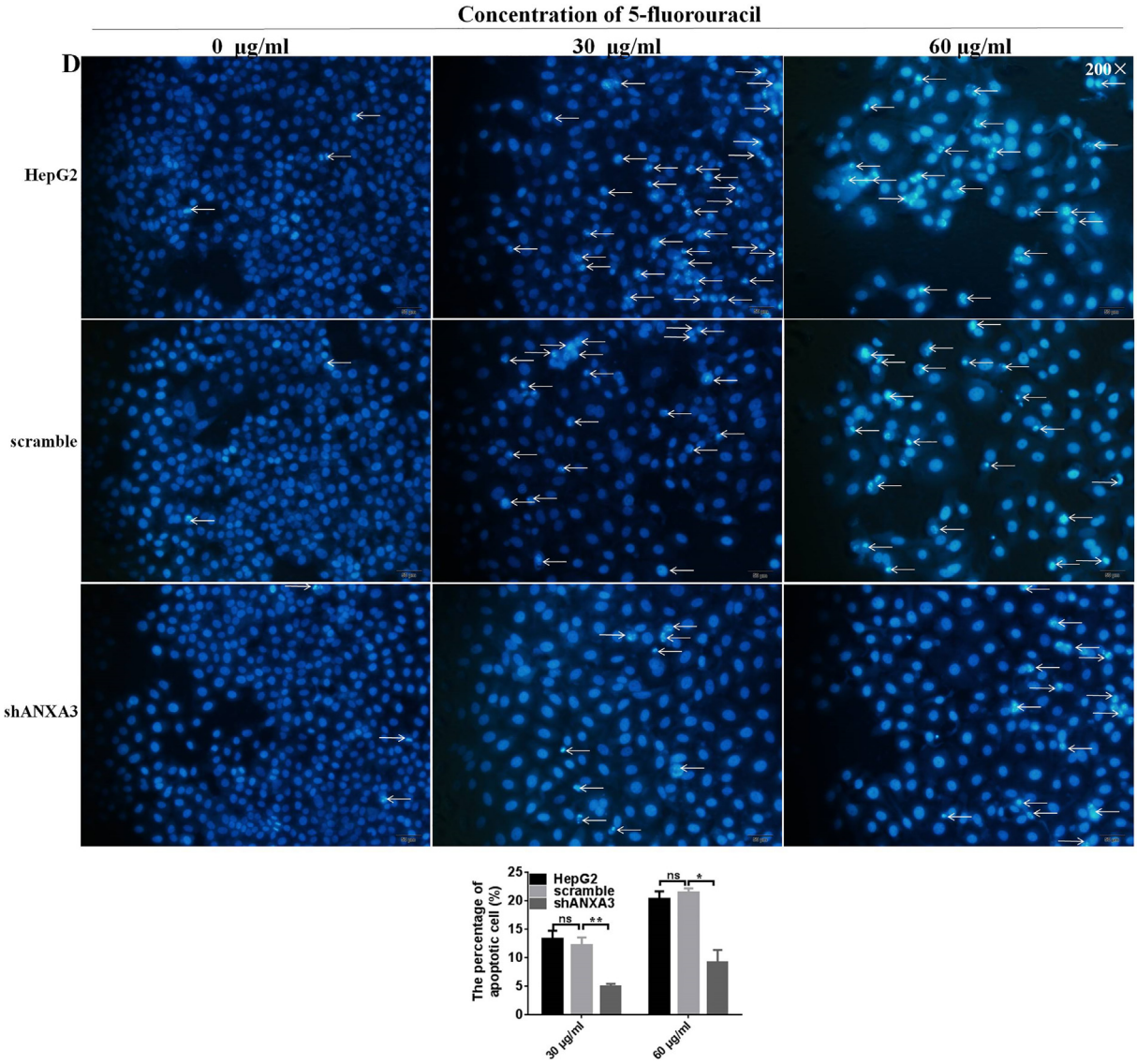

Fig. 6 (*continued*)

shall provide insight into their clinical applications. Herein, we investigated the role of 33-kDa ANXA3 in hepatocarcinoma clinical malignancy and chemo-resistance with the underlying action mechanisms. To our best knowledge, this work is the first report on distinguishing the contribution of 33-kDa ANXA3 in cancer out of total ANXA3.

ANXA3 facilitated the clinical malignancy of gastric cancer [42,35], colorectal cancer [43], lung cancer [36], pancreatic cancer [44] and breast cancer [39,45,46]. ANXA3 overexpression in colorectal cancer tissues correlated with tumor growth and poor prognosis of colorectal cancer patients [43]. ANXA3 upregulation was positively related with the advances of clinical stage, lymphatic metastasis and recurrence of lung adenocarcinoma patients [36]. ANXA3 was upregulated at mRNA level in cancerous tissues from pancreatic cancer patients [44]. The overexpression of ANXA3 in cancerous tissues [45,46] was linked to the enhanced tumor size and lymph node metastasis, and reduced disease-free and overall survivals of breast cancer patients [39,46]. Consistently, current work indicated both 33-kDa and 36-kDa ANXA3 overexpressed in tumorous tissues of hepatocarcinoma patients (Fig. 2) by exhibiting promoting role in hepatocarcinoma carcinogenesis. However, due to the incomplete pathological information of patients and relative small number of patient samples, the expression levels of 33-kDa ANXA3 and 36-kDa ANXA3 were not related to patients' age, gender, TNM stage, HBV and perineuronal invasion. In the future, we will increase the number of patient samples, deeply investigate the expression pattern of 33-kDa ANXA3/36-kDa ANXA3 in hepatocarcinoma and analysis the association of ANXA3 with hepatocarcinoma clinicopathologic parameters.

ANXA3 promoted the *in vitro* malignant properties of tumor cell lines of gastric cancer [35,42], colorectal cancer [47], breast cancer [39,48,49], lung cancer [50] and osteosarcoma [51]. ANXA3 knockdown led to the decreased proliferation, invasion, wound-healing and colony forming abilities of MDA-MB-468, MDA-MB 231 and hepatocarcinoma-1954 cells [38,39]. ANXA3 was upregulated in human gastric epithelium (OTA-GES-1T) cells following ochratoxin (OTA) treatment that enhanced cells' malignant transformation, while, its downregulation effectively suppressed the proliferation and metastasis abilities of OTA-GES-1T [41]. Consistently, the expression level of ANXA3 was reported positively associated with the malignant behaviours of hepatocarcinoma SK-Hep1, SMMC-7721 and Huh7 cell lines [36]. However, without distinguishing the respective functions of two ANXA3 subtypes, only the function of total ANXA3 was linked to hepatocarcinoma malignancy [36].

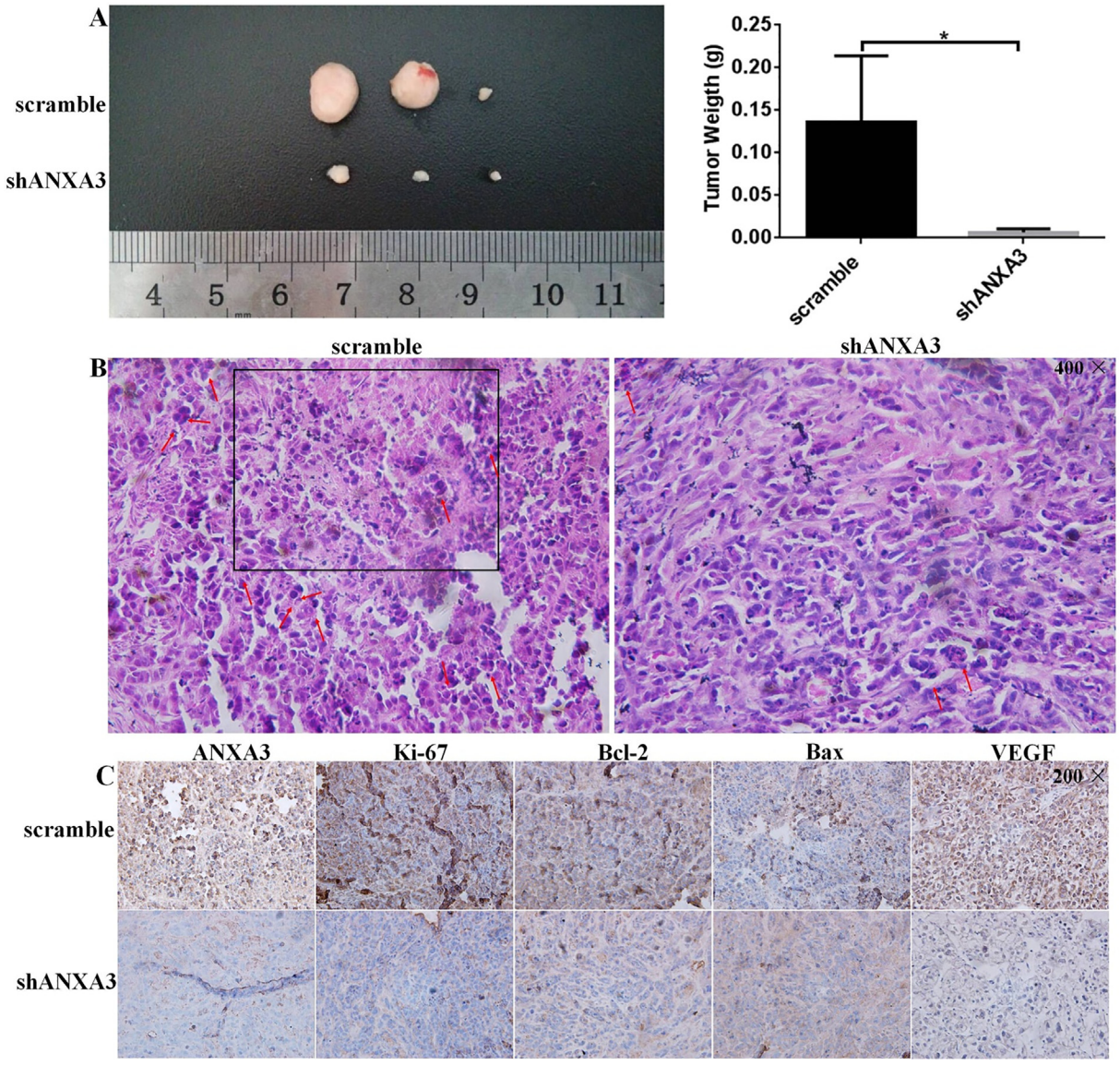

Fig. 7. 33-kDa ANXA3 knockdown suppressed *in vivo* tumorigenesis of HepG2 cell. (**A**) The tumor growth of shANXA3 group cells was reduced compared with scramble group. * refers to $P < 0.05$. HE images of xenografts (**B**) and IHC representative images of Ki-67, Bcl-2, Bax and VEGF in xenografts (**C**) from shANXA3-HepG2-transplanted and scramble-HepG2-transplanted nude mice. The necrosis area was marked with box and apoptotic cells were marked with arrow.

Herein, we specifically revealed the role of 33-kDa ANXA3 in hepatocarcinoma malignancy. As 33-kDa ANXA3 overexpression was correlated with hepatocarcinoma, we proposed its knockdown should antagonize the *in vitro* malignant properties and *in vivo* tumorigenesis of hepatocarcinoma cells. Excitingly and fortunately, we successfully obtained a monoclonal HepG2 cell line with stable specific knockdown of 33-kDa ANXA3 using shRNA interference (Fig. 3A) to appropriately reveal its pure contribution in hepatocarcinoma carcinogenesis. 33-kDa ANXA3 knockdown decreased the *in vitro* proliferation (Fig. 3B), colony formation (Fig. 3C), migration and invasion (Fig. 4) capacities and the *in vivo* tumorigenicity of HepG2 cells (Fig. 7). Apparently, 33-kDa ANXA3 acts as a tumour promoter in hepatocarcinoma development and occurrence. We further showed 33-kDa ANXA3 affected hepatocarcinoma cell's invasiveness through altering cellular F-actin polymerization. Its downregulation resulted in an obvious reduce of F-actin microfilaments in HepG2 cells (Fig. 4C). The cancer cells movement from one position to another site is a complex process requiring dramatic remodeling of cell cytoskeleton where F-actin microfilament is one key component. The abnormal expression or regulation of cytoskeletal components could affect cancer cell metastasis [52–54]. Here, we demonstrated 33-kDa ANXA3 downregulation suppressed hepatocarcinoma cell aggressiveness through reducing F-actin polymerization in cytoskeleton (Fig. 4C). Accordingly, 33-kDa ANXA3 overexpression strengthened cytoskeleton structure in favor of the invasiveness of tumor cells and the malignancy of hepatocarcinoma patients. This work also showed 33-kDa ANXA3 upregulation might promote the growth and invasiveness of cancer cells in hepatocarcinoma through inhibiting their apoptosis. The stable knockdown of 33-kDa ANXA3 promoted both the *in vitro* apoptosis of HepG2 cells at early phase (Fig. 5C) and the *in vivo* apoptosis of cancer cells in primary tumor induced by HepG2-transplantion in nude mice (Fig. 7B). Collectively, 33-kDa ANXA3 acts as a promotor in hepatocarcinoma carcinogenesis. Its upregulation is a potential indicator and biomarker for hepatocarcinoma malignancy.

Angiogenesis supply nutrients and oxygen, and promote the spread of tumour cells for tumor growth and metastasis [28,55,56]. The hypervascular nature of most liver tumors underlines the importance of angiogenesis in their malignancies. VEGF is a

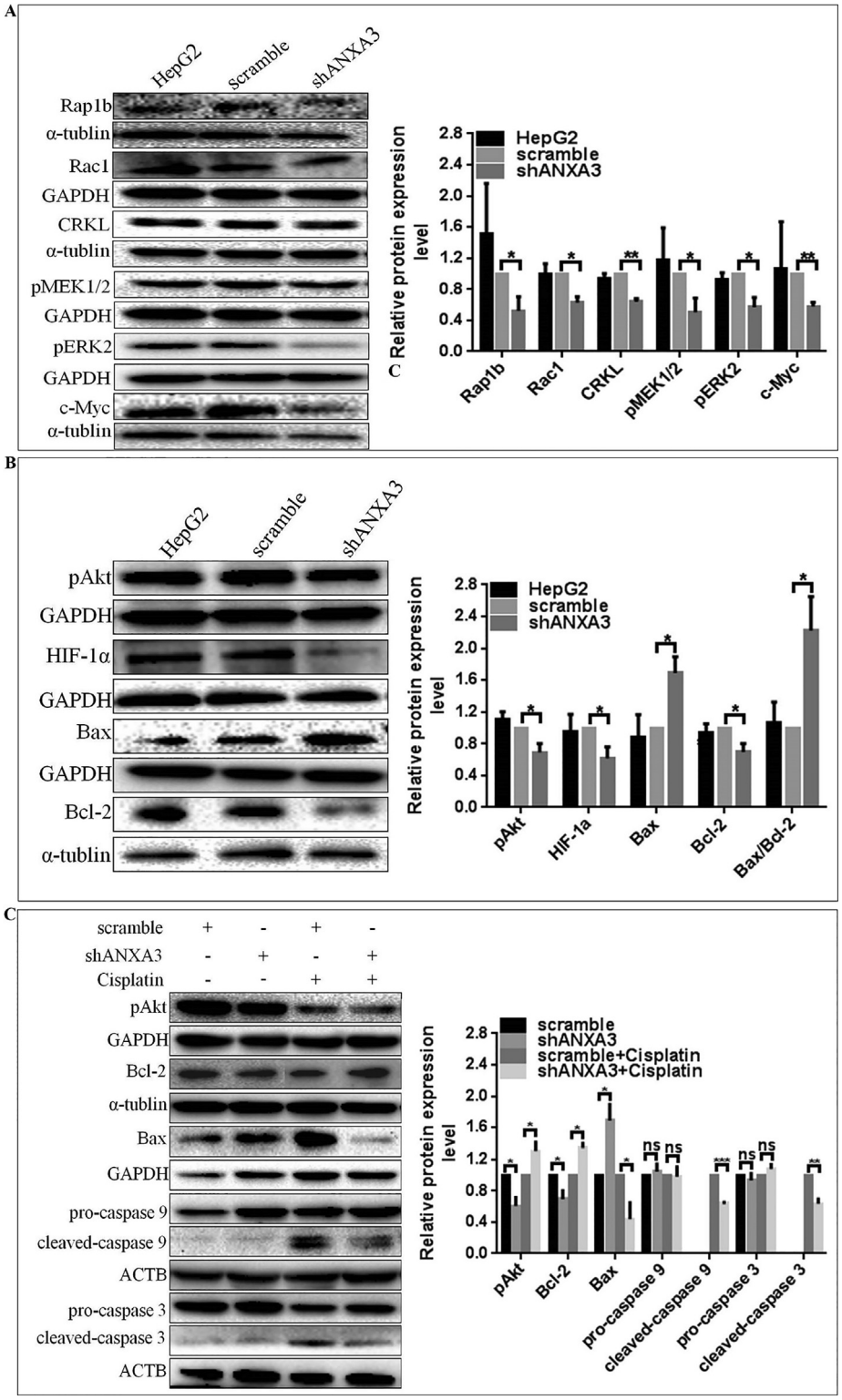

Fig. 8. Molecular regulation mechanism of 33-kDa ANXA3 on hepatocarcinoma cell malignancy. 33-kDa ANXA3 knockdown inhibited (**A**) ERK, (**B**) PI3K/Akt and (**C**) intrinsic apoptotic pathways. *, ** and *** refer to $P < 0.05$, 0.01 and 0.001, ns refers to no statistical difference.

prominent angiogenic factor for supporting the neovascularization of cancer tissue in cancer development [57]. By binding to the hypoxia-responsive element (HRE) of VEGF promoter region, HIF-1, a dimeric transcription factor consisting of HIF-1α and HIF-1β, upregulated the transcription of VEGF [58]. Park et al reported that high level of VEGF was secreted in the conditioned medium obtained from ANXA3-overexpressing HEK 293 cells and higher transactivation activity of HIF-1 was also detected in ANXA3-overexpressing HEK 293 cells, which suggested ANXA3 inducing VEGF production *via* HIF-1 pathway in angiogenesis [28]. Interestingly, in primary cell cultures from RCC patients, 33-kDa ANXA3 upregulation positively correlated, while, 36-kDa ANXA3 downregulation inversely correlated with HIF-1α expression, which showed the total ANXA3 protein was downregulated and negatively corre-

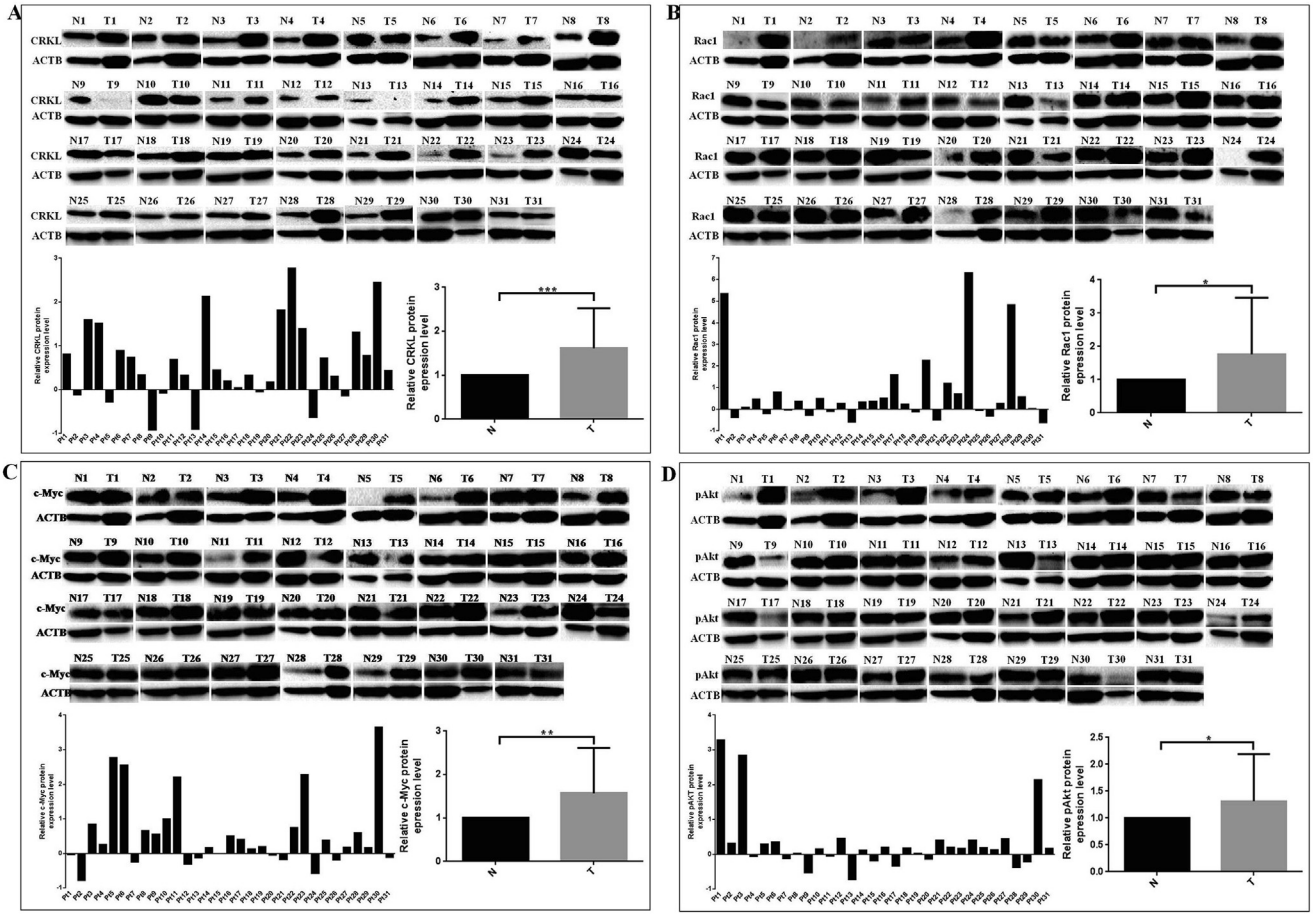

Fig. 9. Expression patterns of CRKL, Rac1, c-Myc and pAkt in hepatocarcinoma tissues. Compared with paracancerous normal liver tissues, the global protein expression levels of (**A**) CRKL, (**B**) Rac1, (**C**) c-Myc, (**D**) pAkt were increased in hepatocarcinoma patients' tumorous tissues. ACTB was the internal reference. *, ** and *** refer to $P < 0.05$, 0.01 and 0.001.

lated with HIF-1α [22]. We also found the level of VEGF was decreased in the TCM obtained from 33-kDa ANXA3 knockdown HepG2 cells (Fig. 5A), indicating VEGF may be the effector for 33-kDa ANXA3-mediated angiogenesis. Furthermore, our work directly linked 33-kDa ANXA3 in hepatocarcinoma angiogenesis through HIF-1α. Its stable knockdown apparently reduced the tube formation ability of HUVE Cinduced by HepG2 cells (Fig. 5B), meanwhile, significantly suppressed the expression of HIF-1α in HepG2 cells (Fig. 8B), moreover, the expression level of VEGF in primary tumor from shANXA3-HepG2-tansplanted mice was lower than that in the scramble-HepG2 group mice (Fig. 7C). Therefore, 33-kDa ANXA3 upregulation contributes to the neovascularization of tumor tissues for supporting the hyperplasia, migration and invasion of hepatocarcinoma cells, which in turn exacerbates hepatocarcinoma malignancy.

Current work showed 33-kDa ANXA3 mediated hepatocarcinoma malignancy through Rac1-ERK pathway.

Actin filaments exist as networks or bundles that are highly regulated by hundreds of proteins. It is commonly reported that the Rho-family of GTPases (RhoA, Rac1 and cdc42) are important regulators of the actin cytoskeleton rearrangement. Rac1 serves as one of the molecular switches formed by the above regulating proteins to relay signals from cell membrane to cytoskeleton in maintaining the formation of the distinct F-actin-based structures. F-Actin microfilaments are important for cell motility, migration and invasion [59,60]. Meanwhile, as a main subfamily of MAPK, ERK pathway plays important roles in proliferation and metastasis of tumor cell [61]. 33-kDa ANXA3 stable knockdown apparently suppressed the expressions of pMEK and pERK2 in HepG2 cells (Fig. 8A). Meanwhile, the expressions of ERK upstream molecules Rap1b, Rac1 and CRKL, and a downstream molecule c-Myc were inhibited in HepG2 cells (Fig. 8A). Correspondingly, CRKL, Rac1 and c-Myc proteins were higher measured in the hepatocarcinoma tumorous tissues compared with paired non-tumor liver tissues (Fig. 8). F-Actin microfilaments are important for cell motility, migration and invasion, 33-kDa ANXA3 upregulation might promote F-actin expression and polymerization in cytoskeleton by regulating Rac1 expression, then promoting tumor cell motility, migration and invasion through activating ERK pathway. 33-kDa ANXA3 upregulation seems to promote hepatocarcinoma cell malignancy by regulating Rac1 expression through activating ERK pathway.

33-kDa ANXA3 mediated the apoptosis and angiogenesis of hepatocarcinoma cells *via* PI3K/Akt pathway. As an important intracellular signaling pathway, PI3K/Akt regulates the cell apoptosis, angiogenesis and metastasis through its downstream effector molecules Bax, Bcl-2, HIF-1α and NF-κβ [62]. The direct binding of SH3N domain of CRKL to the p85 PxxP motif of PI3K resulted in activated PI3K [63] for generating the PIP2 and PIP3 at inner surface of plasma membrane. Then, Akt bond to PIP3 *via* PH domain, simultaneously got phosphorylated at Thr308 by phosphoinositide dependent kinase-1 (PDK1) binding to PIP3, and phosphorylated its downstream target substrates to exhibit diverse biological functions [64]. The increase of expression ratio of Bax/Bcl-2 commonly results in cancer cell apoptosis. ANXA3 could regulate cancer cell apoptosis through altering Bax/Bcl-2 balance [46]. Consistently, our work showed that 33-kDa ANXA3 knockdown

resulted in decreased expressions of CRKL, pAkt and Bcl-2, increased expression of Bax and elevated Bax/Bcl-2 ratio in HepG2 cells (Fig. 8B). Accordingly, pAkt was confirmed significantly overexpressed in the hepatocarcinoma tumorous tissues (Fig. 9). Collectively, 33-kDa ANXA3 knockdown induced apoptosis of HepG2 cells through inactivating PI3K/Akt pathway *via* increasing Bax and decreasing Bcl-2 expressions. Meanwhile, PI3K/Akt/mTOR/HIF-VEGF pathway plays crucial role in angiogenesis. pAkt activated mTOR to enhance HIF-1 transactivation activity and induce VEGF production [65]. ANXA3 was reported to induce angiogenesis through enhancing HIF-1 transactivation activity [28]. 33-kDa ANXA3 knockdown resulted in decreased expression of HIF-1α in HepG2 cells (Fig. 8B) and HepG2-induced tube formation ability of HUVEC cells. Therefore, its knockdown suppressed angiogenesis ability of HepG2 cells through inactivating PI3K/Akt pathway *via* decreasing HIF-1α expression. Pertinent to our study, ANXA3 functioned in angiogenesis for the repair and healing of myocardial cells in rat with acute myocardial infarction through PI3K/Akt pathway [66]. This work shows 33-kDa ANXA3 contributes in hepatocarcinoma malignancy through promoting angiogenesis to support cancer cells *via* activating PI3K/Akt-HIF pathway.

ANXA3 dysexpression is related to the chemoresistances of breast cancer [39], colorectal cancer [67], lung adenocarcinoma [68,69], ovarian cancer [70–72], prostate cancer [73] and hepatocarcinoma [37,74,75]. ANXA3 enhanced the sensitivity of breast cancer cells to doxorubicin [39]. While, ANXA3 upregulation was involved in the increased chemoresistances to oxaliplatin (Ox) in colorectal cancer HCT116/Ox and SW480/Ox cells [67], to cisplatin in lung cancer A549, H661 and SK-MES-1cells [69], to cisplatin and carboplatin in ovarian cancer SKOV3 and A2780 cells [71], and even to platinum-resistant ovarian cancer patients than platinum-sensitive patients [72]. Accordingly, ANXA3 knockdown in above cancer cell lines increased their sensitivities to these reagents [67,69,71,72]. In hepatocarcinoma, the upregulation of total ANXA3 was reported to increase the resistances of SK-Hep1 and SMMC7721 cells to cisplatin and 5-FU, and to enhance chemoresistance in nude mice; while, its knockdown decreased the resistances of Huh7 cells to cisplatin and 5-FU [37]. What is the role of 33-kDa ANXA3 in drug resistance of hepatoma cells? We showed 33-kDa ANXA3 deregulation was involved in the chemosensitivities of HepG2 cells. Its knockdown enhanced HepG2 resistances to cisplatin and 5-FU (Fig. 6). While, total ANXA3 was previously reported to enhance the chemoresistances of hepatocarcinoma SK-Hep1 and SMMC7721 cells to cisplatin and 5-FU [37], although the difference may be caused as different hepatocarcinoma cell lines being used, this also implicated that 33-kDa ANXA3 and 36-kDa ANXA3 might function differently in chemosensitivity of hepatocarcinoma cells, which deserves more attention to distinguish the distinction between the two ANXA3 isoforms. Current work found 33-kDa ANXA3 knockdown in HepG2 increased its IC_{50} to cisplatin by 62.3% and to 5-FU by 83.5%, respectively, conferred HepG2 cells more resistant to cisplatin than to 5-FU (Fig. 6A). We further showed that 33-kDa ANXA3 mediated HepG2 sensitivity to cisplatin through intrinsic apoptotic pathway. With the treatment of cisplatin (2 μg/ml), the protein expression levels of pAkt and Bcl-2 were higher, while, Bax, cleaved caspase 9 and cleaved caspase 3 were lower detected in shANXA3-HepG2 cells compared with the scramble group HepG2 cells (Fig. 8C). Bax upregulation and Bcl-2 downregulation accelerated Cytochrome *c* release from mitochondria into cytoplasm. Then, the cytosolic Cytochrome *c* bond with Apaf-1 to form a large complex apoptosome that first recruited and activated pro-caspase 9 to produce cleaved-caspase 9, then recruited and activated pro-caspase 3 to produce cleaved-caspase 3, and finally blocked DNA damage repair and induced apoptosis [76,77]. Therefore, 33-kDa ANXA3 downregulation enhanced HepG2 cell chemoresistance *via* inactivating the intrinsic apoptotic pathway.

Apoptosis or programmed cell death, is an essential cell process in homeostasis of multicellular organisms, including early apoptosis and late apoptosis [78]. Late apoptosis is closer to necrosis, so it is also called secondary necrosis. Strict regulation of apoptosis is widely involved in many human diseases, including cancers [79]. The therapeutical strategy targeting the early apoptosis of cancer cells is listed among the most successful non-surgical treatment, as the apoptosis evasion is a hallmark of cancer and is nonspecific to cancer type. Hence, many anticancer drugs have been produced through the actions on targeting genes involved in both the intrinsic and extrinsic pathways [80]. This work showed that 33-kDa ANXA3 downregulation promoted the early apoptosis of HepG2 cells, which implicated its potential application in inhibiting carcinogenesis by promoting the early apoptosis of tumor cells to therapy cancer at early phase. We may continue investigating the influence 33-kDa ANXA3 downregulation on the cell cycle and apoptosis of tumor cells with the underlying mechanism, which will provide fundamental basis for the practical application of 33-kDa ANXA3 in the clinical treatment of hepatocarcinoma even other cancers. In the future, appropriate anticancer drugs will directly target 33-kDa ANXA3 to treat cancer at early stage and may improve cure rate. Molecule-targeted therapy will gradually become a new favorite for treatment of cancer, and also represent the future developmental direction of treatment of cancer. Furthermore, fundamental research breakthroughs will create more effective methods for cancer targeted therapy.

Conclusion

Taken together, our study illuminates, for the first time, that 33-kDa ANXA3 isoform presenting tumor promoting effect on the malignant behaviours of HepG2 cells. 33-kDa ANXA3 downregulation inhibited proliferation, colony formation, migration and invasion of HepG2 cells *via* inhibiting ERK pathway. 33-kDa ANXA3 downregulation inhibited angiogenesis of HepG2 cells *via* inhibiting PI3K/Akt-HIF pathway. 33-kDa ANXA3 downregulation promoted apoptosis and enhanced HepG2 chemoresistance *via* inactivating the intrinsic apoptotic pathway. The potential action mechanism was outlined in Fig. 10. (1) 33-kDa ANXA3 upregulates CRKL and Rap1b expressions to activate the expressions of downstream molecules Rac1, pMEK1/2, pERK2 and c-Myc in promoting the proliferation, colony formation, migration and invasion abilities of HepG2 cells; (2) The binding with CRKL activates PI3K to generat PIP3 at the inner membrane, to recruit Akt through binding to PIP3 and get Akt phosphorylated at Thr308 by PDK1 through its binding to PIP3. Subsequently pAkt activates mTOR to enhance HIF-1α transactivation activity, HIF-1α/HIF-1β bind to the HRE of VEGF promoter region to induce VEGF production, then 33-kDa ANXA3 promoted angiogenesis of HepG2 cells through activating PI3K/Akt *via* increasing HIF-1α expression; (3) Furthermore, pAkt decreases Bax and increases Bcl-2 expressions, Bax upregulation and Bcl-2 downregulation promoted cytochrome *c* release from mitochondria into the cytoplasm, then binds to Apaf-1 and forms apoptosome to recruits and activates pro-caspase 9, following by pro-caspase 3 cleavage and activation, cleaved-caspase 9 and cleaved-caspase 3 blocked DNA damage repair to induce apoptosis, then 33-kDa ANXA3 inhibited HepG2 cells apoptosis and chemoresistance *via* activating caspase 9 and caspase 3. In conclusion, 33-kDa ANXA3 plays an oncogenic role in hepatocarcinoma, it may be a novel potential indicator and biomarker for the malignant progression and therapeutic target for diagnosis and treatment of hepatocarcinoma.

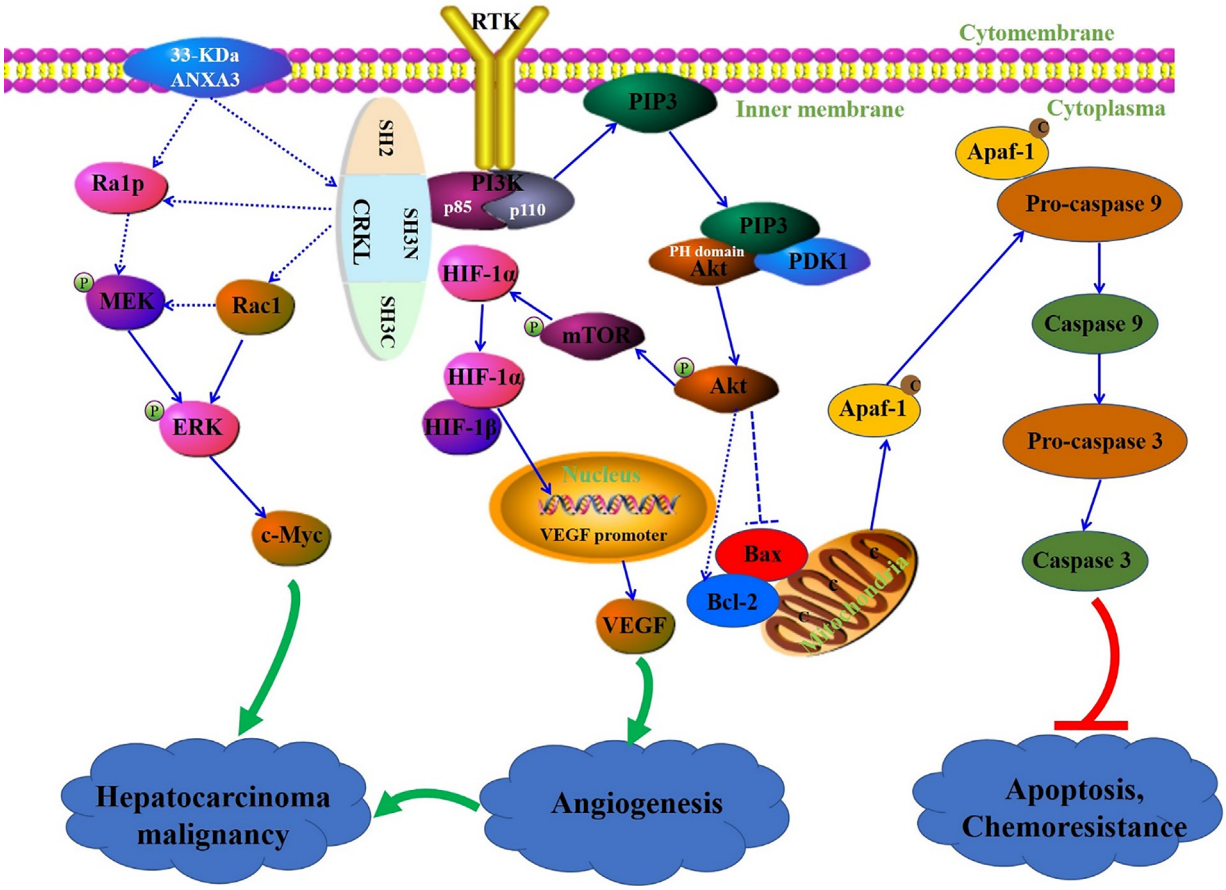

Fig. 10. The potential action mechanism of 33-kDa ANXA3 on hepatocarcinoma malignancy. 33-kDa ANXA3 1) promotes proliferation, colony formation, migration and invasion abilities of hepatocarcinoma cell *via* activating ERK pathway, 2) promotes angiogenesis of hepatocarcinoma cell *via* activating PI3K/Akt-HIF pathway, 3) inhibits apoptosis and chemoresistance of hepatocarcinoma cell *via* activating intrinsic apoptotic pathway. represents non-direct activation action between genes, represents non-direct inhibition between genes, represents direct activation action between genes, represents promotion effect, represents inhibition effect.

Compliance with ethics requirements

All Institutional and National Guidelines for the care and use of animals (fisheries) were followed.

All procedures followed were in accordance with the ethical standards of the responsible committee on human experimentation (institutional and national) and with the Helsinki Declaration of 1975, as revised in 2008 (5). Informed consent was obtained from all patients for being included in the study.

Acknowledgements

This work was supported by grants from National Natural Science Foundation of China (31900517, 81272186, 81672737) and Natural Science Foundation of Liaoning (LQ2017001, 20181550168, LZ2019003, LZ2020045) and Liaoning Provincial Program for Top Discipline of Basic Medical Sciences.

Authors' contributions

CMG, NNL and CYD designed the experiments; CMG, NNL, ZPL and CYD performed *in vitro* experiments; CMG and NNL performed the *in vivo* experiments; LMW and QLL organized the clinical samples; QLM, TYX and LHH analyzed the data; CMG wrote the manuscript; SQL, MZS and FTG modified the manuscript. All authors read and approved the final manuscript.

Ethics approval and consent to participate

The mice were provided by the SPF Experimental Animal Center of Dalian Medical University, mice were maintained under standard conditions and treated according to the institutional guidelines of laboratory animals, all animal experiments were approved by the Experimental Animal Ethical Committee of Dalian Medical University (Permit Number: AAE18064); Tissue study protocols were approved by the Medical Ethics Committee of Dalian Medical University with approval number 2019-014, all experiment methods were carried out according to the relevant guidelines and regulations.

Declaration of Competing Interest

The authors declare that they have no competing interests.

References

[1] Siege RL, Miller KD, Jemal A. Cancer statistics. Can J Clin 2019;69(1):7–34.
[2] El-Serag HB, Rudolph KL. Hepatocarcinoma: epidemiology and molecular carcinogenesis. Gastroenterology 2017;132(7):2557–76.
[3] Alqahtani A, Khan Z, Alloghbi A, Said Ahmed TS, Ashraf M, Hammouda DM. Hepatocarcinoma: molecular mechanisms and targeted therapies. Medicina 2019;155(9):526.
[4] Aravalli RN, Steer CJ, Cressman EN. Molecular mechanisms of hepatocarcinoma. Hepatology 2008;48(6):2047–63.
[5] Koerdt SN, Ashraf APK, Gerke V. Annexins and plasma membrane repair. Curr Top Membr 2019;84:43–65.
[6] Anuphon L, Julia MD. Annexins. New Phytol 2011;189(1):40–53.

[7] Theresa LB, Jesper N. Annexins in plasma membrane repair. Biol Chem 2016;397(10):961–9.
[8] Rescher U, Grewal T. Highlight: annexins in health and disease. Biol Chem 2016;397(10):947–8.
[9] Purvis GSD, Solito E, Thiemermann C. Annexin-A1: Therapeutic potential in microvascular disease. Front Immunol 2019;10:938.
[10] Gerke V, Moss SE. Annexins: from structure to function. Physiol Rev 2002;82 (2):331–71.
[11] Mussunoor S, Murray GI. The role of annexins in tumor development and progression. J Pathol 2008;216:131–40.
[12] Rescher U, Gerke V. Annexins-unique membrane binding proteins with diverse functions. Cell Sci 2004;117(13):2631–9.
[13] Hayes MJ, Moss SE. Annexins and disease. Biochem Biophys Res Commun 2004;322(4):1166–70.
[14] Sun X, Liu S, Wang J, Wei B, Guo C, Chen C, et al. Annexin A5 regulates hepatocarcinoma malignancy *via* CRKI/II-DOCK180-RAC1 integrin and MEK-ERK pathways. Cell Death Dis 2018;9(6):637.
[15] Qi H, Liu S, Guo C, Wang J, Greenaway FT, Sun M-Z. Role of annexin A6 in cancer. Oncol Lett 2015;10(4):1947–52.
[16] Wei B, Guo C, Liu S, Sun M-Z. Annexin A4 and cancer. Clin Chim Acta 2015;447:72–8.
[17] Wang J, Guo C, Liu S, Qi H, Yin Y, Liang R, et al. Annexin A11 in disease. Clin Chim Acta 2014;431:164–8.
[18] Peng B, Guo C, Guan H, Liu S, Sun M-Z. Annexin A5 as a potential marker in tumors. Clin Chim Acta 2014;427:42–8.
[19] Guo C, Liu S, Sun M-Z. Potential role of Anxa1 in cancer. Future Oncol 2013;9 (11):1773–93.
[20] Guo C, Liu S, Greenaway FT, Sun M-Z. Potential role of annexin A7 in cancer. Clin Chim Acta 2013;423:83–9.
[21] Zhang X, Liu S, Guo C, Zong J, Sun M-Z. The association of annexin A2 and cancers. Clin Transl Oncol 2012;14(9):634–40.
[22] Le Cabec V, Russo-Marie F, Maridonneau-Parini I. Differential expression of two forms of annexin A3 in human neutrophils and monocytes and along their differentiation. Biochem Biophys Res Commun 1992;189(3):1471–6.
[23] Bianchi C, Bombelli S, Raimondo F, Torsello B, Angeloni V, Ferrero S, et al. Primary cell cultures from human renal cortex and renal-cell carcinoma evidence a differential expression of two spliced isoforms of annexin A3. Am J Pathol 2010;176(4):1660–70.
[24] Perron B, Lewit-Bentley A, Geny B, Russo-Marie F. Can enzymatic activity, or otherwise, be inferred from structural studies of Annexin III?. J Biol Chem 1997;272:11321–6.
[25] Sopkova J, Raguenes NC, Vincent M, Chevalier A, Lewit BA, Russo MF, et al. Ca (2+) and membrane binding to annexin 3 modulate the structure and dynamics of its N terminus and domain III. Protein Sci 2002;11(7):1613–25.
[26] Hofmann A, Raguenes-Nicol C, Favier-Perron B, Mesonero J, Huber R, Russo-Marie F, et al. The annexin A3 membrane interaction is modulated by an N-terminal tryptophan. Biochem 2000;39(26):7712–21.
[27] Wu N, Liu S, Guo C, Hou Z, Sun M-Z. The role of annexin A3 playing in cancers. Clin Transl Oncol 2013;15(2):106–10.
[28] Park JE, Lee DH, Lee JA, Park SG, Kim NS, Park BC, et al. Annexin A3 is a potential angiogenic mediator. Biochem Biophys Res Commun 2005;337 (4):1283–7.
[29] Meadows SM, Cleaver O, Ondine C. Annexin A3 regulates early blood vessel formation. PLoS ONE 2015;10(7):e0132580.
[30] ShingoN Mizuho H, Masaru G, Masashi H, Taiichiro S, Toyohiko A, et al. Expression of annexin A3 in primary cultured parenchymal rat hepatocytes and inhibition of DNA synthesis by suppression of annexin A3 expression using RNA interference. Biol Pharm Bull 2005;28(3):424–8.
[31] Harashima M, Nimi S, Koyanagl H, Hyuga M, Noma S, Seki T, et al. Change in annexin A3 expression by regulatory factors of hepatocyte growth in primary cultured rat hepatocytes. Biol Pharm Bull 2006;29(7):1339–43.
[32] Wozny W, Schroer K, Schwall GP, Poznanovic S, Stegmann W, Dietz K, et al. Differential radioactive quantification of protein abundance ratios between benign and malignant prostate tissues: cancer association of annexin A3. Proteomics 2007;7:313–22.
[33] Schostak M, Schwall GP, Poznanovic S, Groebe K, Muller M, Messinger D, et al. Annexin A3 in urine: a highly specific noninvasive marker for prostate cancer early detection. J Urol 2009;181(1):343–53.
[34] Kollermann J, Schlomm T, Bang H, Schwall GP, von Eichel-Streiber C, Simon R, et al. Expression and prognostic relevance of annexin A3 in prostate cancer. Eur Urol 2008;54(6):1314–23.
[35] Yu S, Li Y, Fan L, Zhao Q, Tan B, Liu Y. Impact of annexin A3 expression in gastric cancer cells. Neoplasma 2014;61(3):257–64.
[36] Liu Y, Xiao Z, Li M, Li M, Zhang P, Li C, et al. Quantitative proteome analysis reveals annexin A3 as a novel biomarker in lung adenocarcinoma. J Pathol 2009;217(1):54–64.
[37] Pan Q, Pan K, Weng D, Zhao J, Zhang X, Wang D, et al. Annexin A3 promotes tumorigenesis and resistance to chemotherapy in hepatocarcinoma. Mol Carcinogen 2015;54(8):598–607.
[38] Tong M, Fung TM, Luk ST, Ng KY, Lee TK, Lin C, et al. ANXA3/JNK signaling promotes self-renewal and tumor growth, and its blockade provides a therapeutic target for hepatocarcinoma. Stem Cell Rep 2015;5(1):45–59.
[39] Du R, Liu B, Zhou L, Wang D, He X, Xu X, et al. Downregulation of annexin A3 inhibits tumor metastasis and decreases drug resistance in breast cancer. Cell Death Dis 2018;9(2):126.
[40] Kim JY, Jung EJ, Park HJ, Lee JH, Song E, Kwag SJ, et al. Tumor-suppressing effect of silencing of annexin A3 expression in breast cancer. Clin Breast Can 2018;18 (4):e713–9.
[41] Junker H, Suofu Y, Venz S, Sascau M, Herndon JG, Kessler C, et al. Proteomic identification of an upregulated isoform of Annexin A3 in the rat brain following reversible cerebral ischemia. Glia 2007;55:1630–7.
[42] Wang J, Jia X, Meng X, Li Y, Wu W, Zhang X, et al. Annexin A3 may play an important role in ochratoxin-induced malignant transformation of human gastric epithelium cells. Toxicol Lett 2019;313:150–8.
[43] Xie Y, Fu D, He Z, Tan Q. Prognostic value of Annexin A3 in human colorectal cancer and its correlation with hypoxia-inducible factor-1α. Oncol Lett 2013;6 (6):1631–5.
[44] Baine MJ, Chakraborty S, Smith LM, Mallya K, Sasson AR, Brand RE. Transcriptional profiling of peripheral blood mononuclear cells in pancreatic cancer patients identifies novel genes with potential diagnostic utility. PLoS ONE 2011;6(2):e17014.
[45] Zhou T, Liu L, Yang L. The expression of ANXA3 and its relationship with the occurrence and development of breast cancer. J BUON 2018;23(3):713–9.
[46] Zeng C, Ke ZF, Song Y, Yao Y, Hu X, Zhang M, et al. Annexin A3 is associated with a poor prognosis in breast cancer and participates in the modulation of apoptosis *in vitro* by affecting the Bcl-2/Bax balance. Exp Mol Pathol 2013;95 (1):23–31.
[47] Li X, Hu W, Yu J, Zheng S. Inhibition of annexin A3 suppresses cell proliferation and aggressiveness in colorectal cancer. Clin Gastroenterol Hepatol 2017;15 (1):e50.
[48] Zhou T, Li Y, Yang L, Liu L, Ju Y, Li C. Silencing of ANXA3 expression by RNA interference inhibits the proliferation and invasion of breast cancer cells. Oncol Rep 2017;37(1):388–98.
[49] Li J, Zhou T, Liu L, Ju Y, Chen Y, Tan Z, et al. The regulatory role of Annexin 3 in a nude mouse bearing a subcutaneous xenograft of MDA-MB-231 human breast carcinoma. Pathol Res Pract 2018;214(10):1719–25.
[50] Liu Y, Liu Q, Zhang Y, Qiu J. Annexin A3 knockdown suppresses lung adenocarcinoma. Anal Cell Pathol 2016;2016:4131403.
[51] Zeng X, Wang S, Gui P, Wu H, Li Z. Expression and significance of Annexin A3 in the osteosarcoma cell lines HOS and U2OS. Mol Med Rep 2019;20(3):2583–90.
[52] Small JV, Stradal T, Vignal E, Rottner K. The lamellipodium: where motility begins. Trends Cell Biol 2002;12(3):112–20.
[53] Pollard TD, Borisy GG. Cellular motility driven by assembly and disassembly of actin filaments. Cell 2003;112(4):453–65.
[54] Ridley AJ, Schwartz MA, Burridge K, Firtel RA. Ginsberg MH, Borisy G. Cell migration: integrating signals from front to back. Science. 2003; 302 (5651): 1704–9.
[55] Huang X, Huang Z, Huang J, Xu B, Huang X, Xu Y, et al. Exosomal circRNA-100338 promotes hepatocarcinoma metastasis *via* enhancing invasiveness and angiogenesis. J Exp Clin Cancer Res 2020;39(1):20–35.
[56] Zhang Q, Lu S, Li T, Yu L, Zhang Y, Zeng H, et al. ACE2 inhibits breast cancer angiogenesis *via* suppressing the VEGFa/VEGFR2/ERK pathway. J Exp Clin Can Res 2019;38(1):173–84.
[57] Loureiro RM, D'Amore PA. Transcriptional regulation of vascular endothelial growth factor in cancer. Cytokine Growth Factor Rev. 2005; 16 (1): 77–89.
[58] Cho S, Choi YJ, Kim JM, Jeong ST, Kim JH, Kim SH, et al. Binding and regulation of HIF-1alpha by a submit of the proteasome complex, PSMA7. FEBS Lett 2001;498(1):62–6.
[59] Nobes CD, Hall A. Rho, rac, and cdc42 GTPases regulate the assembly of multimolecular focal complexes associated with actin tress fibers, lamellipodia, and filopodia. Cell 1995;81:53–62.
[60] Moorman JP, Luu D, Wickham J, Bobak DA, Hahn CS. A balance of signaling by Rho family small GTPases RhoA, Rac1 and Cdc42 coordinates cytoskeletal morphology but not cell survival. Oncogene 1999;18:47–57.
[61] Morrison DK. MAP kinase pathways. Cold Spring Harb Perspect Biol 2012;4 (11):a011254.
[62] Chang F, Lee JT, Navolanic PM, Steelman LS, Shelton JG, Blalock WL, et al. Involvement of PI3K/Akt pathway in cell cycle progression, apoptosis, and neoplastic transformation: a target for cancer chemotherapy. Leukemia 2003;17(3):590–603.
[63] Reorganization of the host cell Crk(L)-PI3 kinase signaling complex by the influenza A virus NS1 protein. Virology 2015;484:146–52.
[64] Rai SN, Dilnashin H, Birla H, Singh SS, Zahra W, Rathore AS, et al. The role of PI3K/Akt and ERK in neurodegenerative disorders. Neurotox Res. 2019;35 (3):775–95.
[65] Shen KK, Ji LL, Gong CY. Notoginsenoside Ft1 promotes angiogenesis via HIF-1 alpha mediated VEGF secretion and the regulation of PI3K/AKT and Raf/MEK/ERK signaling pathways. Biochem Pharmacol 2012;84(6):784–92.
[66] Meng H, Zhang Y, An S, Chen Y. Annexin A3 gene silencing promotes myocardial cell repair through activation of the PI3K/Akt signaling pathway in rats with acute myocardial infarction. J Cell Physiol 2019;234(7):10535–46.
[67] Xu R, Yin J, Zhang Y, Zhang S. Annexin A3 depletion overcomes resistance to oxaliplatin in colorectal cancer *via* the MAPK signaling pathway. J Cell Biochem 2019;120(9):14585–93.
[68] Wang C, Xiao Q, Li Y, Zhao C, Jia N, Li R, et al. Regulatory mechanisms of annexin-induced chemotherapy resistance in cisplatin resistant lung adenocarcinoma. Asian Pac J Can Prev 2014;15(7):3191–4.
[69] Wang L, Li X, Ren Y, Geng H, Zhang Q, Cao L, et al. Cancer-associated fibroblasts contribute to cisplatin resistance by modulating ANXA3 in lung cancer cells. Cancer Sci 2019;110(5):1609–20.

[70] Yan X, Pan L, Yuan Y, Lang J, Mao N. Identification of platinum-resistance associated proteins through proteomic analysis of human ovarian cancer cells and their platinum resistant sublines. J Proteome Res 2007;6(2):772–80.
[71] Yan X, Yin J, Yao H, Mao N, Yang Y, Pan L. Increased expression of annexin A3 is a mechanism of platinum resistance in ovarian cancer. Can Res 2010;70 (4):1616–24.
[72] Yin J, Yan X, Yao X, Zhang Y, Shan Y, Mao N, et al. Secretion of annexin A3 from ovarian cancer cells and its association with platinum resistance in ovarian cancer patients. J Cell Mol Med 2012;16(2):337–48.
[73] Thoenes L, Hoehn M, Kashirin R, Ogris M, Arnold GJ, Wagner E, et al. *In vivo* chemoresistance of prostate cancer in metronomic cyclophosphamide therapy. J Proteomics 2010;73(7):1342–54.
[74] Tong S, Yang Y, Hu H, An X, Ye F, Hu P, et al. Proteomic investigation of 5-fluorouracil resistance in a human hepatocarcinoma cell line. J Cell Biochem 2012;113(5):1671–80.
[75] Tong M, Che N, Zhou L, Luk ST, Kau PW, Chai S, et al. Efficacy of annexin A3 blockade in sensitizing hepatocarcinoma to sorafenib and regorafenib. J Hepatol 2018;69(4):826–39.
[76] Hu Q, Wu D, Chen W, Yan Z, Shi Y. Proteolytic processing of the caspase-9 zymogen is required for apoptosome-mediated activation of caspase-9. J Biol Chem 2013;288(21):15142–7.
[77] Shakeri R, Kheirollahi A, Davoodi J. Apaf-1: Regulation and function in cell death. Biochimie 2017;135:111–25.
[78] Mohamed MS, Bishr MK, Almutairi FM, Ali AG. Inhibitors of apoptosis: clinical implications in cancer. Apoptosis 2017;22(12):1487–509.
[79] Anthony L. Apoptosis and cancer. Can Biol 2017;1:275–94.
[80] Pfeffer CM, Singh Amareshwar TK. Apoptosis: a target for anticancer therapy. Int J Mol Sci 2018;19(2):448.